BIOLOGY OF REPRODUCTION **78,** 1139–1152 (2008)
Published online before print 23 January 2008.
DOI 10.1095/biolreprod.107.062679

Gamendazole, an Orally Active Indazole Carboxylic Acid Male Contraceptive Agent, Targets HSP90AB1 (HSP90BETA) and EEF1A1 (eEF1A), and Stimulates *Il1a* Transcription in Rat Sertoli Cells[1]

Joseph S. Tash,[2,4,5] Ramappa Chakrasali,[6] Sudhakar R. Jakkaraj,[6] Jennifer Hughes,[4] S. Kendall Smith,[4,5] Kaori Hornbaker,[4] Leslie L. Heckert,[4,5] Sedide B. Ozturk,[7] M. Kyle Hadden,[6] Terri Goss Kinzy,[5,7] Brian S.J. Blagg,[5,6] and Gunda I. Georg[3,5,6]

Department of Molecular and Integrative Physiology[4] and Interdisciplinary Center for Male Contraceptive Research and Drug Development,[5] University of Kansas Medical Center, Kansas City, Kansas 66160
Department of Medicinal Chemistry,[6] University of Kansas, Lawrence, Kansas 66045-7582
Department of Molecular Genetics, Microbiology, and Immunology,[7] UMDNJ Robert Wood Johnson Medical School, Piscataway, New Jersey 08854-5635

ABSTRACT

Gamendazole was recently identified as an orally active antispermatogenic compound with antifertility effects. The cellular mechanism(s) through which these effects occur and the molecular target(s) of gamendazole action are currently unknown. Gamendazole was recently designed as a potent orally active antispermatogenic male contraceptive agent. Here, we report the identification of binding targets and propose a testable mechanism of action for this antispermatogenic agent. Both HSP90AB1 (previously known as HSP90beta [heat shock 90-kDa protein 1, beta]) and EEF1A1 (previously known as eEF1A [eukaryotic translation elongation factor 1 alpha 1]) were identified as binding targets by biotinylated gamendazole (BT-GMZ) affinity purification from testis, Sertoli cells, and ID8 ovarian cancer cells; identification was confirmed by matrix-assisted laser desorption/ionization-time of flight mass spectrometry and Western blot analysis. BT-GMZ bound to purified yeast HSP82 (homologue to mammalian HSP90AB1) and EEF1A1, but not to TEF3 or HBS1, and was competed by unlabeled gamendazole. However, gamendazole did not inhibit nucleotide binding by EEF1A1. Gamendazole binding to purified *Saccharomyces cerevisiae* HSP82 inhibited luciferase refolding and was not competed by the HSP90 drugs geldanamycin or novobiocin analogue, KU-1. Gamendazole elicited degradation of the HSP90-dependent client proteins AKT1 and ERBB2 and had an antiproliferative effect in MCF-7 cells without inducing HSP90. These data suggest that gamendazole may represent a new class of selective HSP90AB1 and EEF1A1 inhibitors. Testis gene microarray analysis from gamendazole-treated rats showed a marked, rapid increase in three interleukin 1 genes and *Nfkbia* (*NF-kappaB inhibitor alpha*) 4 h after oral administration. A spike in *Il1a* transcription was confirmed by RT-PCR in primary Sertoli cells 60 min after exposure to 100 nM gamendazole, demonstrating that Sertoli cells are a target. AKT1, NFKB, and interleukin 1 are known regulators of the Sertoli cell-spermatid junctional complexes. A current model for gamendazole action posits that this pathway links interaction with HSP90AB1 and EEF1A1 to the loss of spermatids and resulting infertility.

fertilization, male contraception, Sertoli cells, spermatogenesis, testis

INTRODUCTION

The National Institutes of Health, Institute of Medicine, and World Health Organization have focused attention on the need for novel strategies to develop new nonsteroidal reversible male contraceptives, in part because traditional approaches have yielded mixed results, problems with reversibility, and/or unacceptable side effects [1–3]. A common feature of these appeals for new approaches to male contraception is the need to identify novel protein targets that can be exploited to develop novel chemical structures as male contraceptive agents.

In this regard, our recent success with the development of the novel male contraceptive candidate, gamendazole [4], stemmed from previous work on a class of small indazole carboxylic acids (ICAs) that severely inhibit spermatogenesis and are reversible in rats, mice, rabbits, dogs, and nonhuman primates [5, 6]. This class of compounds exerts its contraceptive effect by eliciting premature release of spermatids via disruption of the Sertoli cell-spermatid junctions, but neither the drug-binding targets nor the precise mechanism by which this occurs have been determined [7]. Because gamendazole is the most potent ICA relative to previously reported ICAs [4, 8, 9], this compound offers the possibility to discover the binding targets and the mechanism of action that account for the loss of spermatogenesis and, thus, its contraceptive effect. Here, we report the successful use of proteomic and reverse genetic approaches to identify several protein-binding targets for gamendazole. Because neither a mechanism of action for gamendazole nor its targets have been determined, we chose gene microarray in testis, focusing on early time points to distinguish early from late response genes, as an initial approach to identify target genes of interest for further study. Using gene microarray technologies in testis and primary Sertoli cells, we identified rapid changes in the transcription of genes regulated by the targets of gamendazole that, in turn, are

[1]Supported by National Institutes of Health (NIH) U54 HD-055763 (to J.S.T.), NIH N01-HD-1–3313 (to G.I.G.), and U54 HD33994 Center for Reproductive Sciences, a National Institute of Child Health and Human Development (NICHD) Grant for Specialized Cooperative Centers Program in Reproductive Research (SCCPRR), at the University of Kansas Medical Center. Also supported by NICHD contract N01-HD-6–3259 awarded to BIOQUAL, Inc. Dedicated to the memory of Geoffrey M.H. Waites, Sc.D., Ph.D., and Thaddeus R.R. Mann, M.D., Ph.D., Sc.D., F.R.S.
[2]Correspondence: FAX: 913 588 7180; e-mail, jtash@kumc.edu
[3]Current address: Department of Medicinal Chemistry, 717 Delaware Street SE, University of Minnesota, Minneapolis, MN 55414.

Received: 9 May 2007.
First decision: 11 July 2007.
Accepted: 7 January 2008.

ISSN: 0006-3363. http://www.biolreprod.org

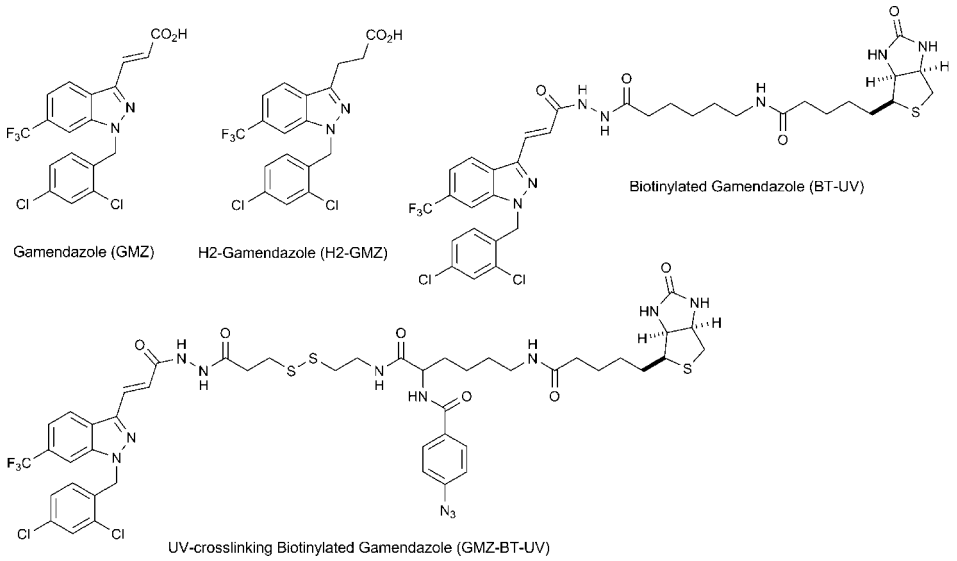

FIG. 1. Structure of gamendazole, H2-gamendazole, biotinylated gamendazole, and biotinylated gamendazole with a UV cross-linking moiety.

known to regulate the integrity of the Sertoli cell-spermatid junctional complexes. Based on these initial observations, we propose a testable model for the mechanism of action of gamendazole in Sertoli cells that explains the protein and molecular pathways leading to its disruption of spermatogenesis and its contraceptive effect. The proposed mechanism of action can form a basis for further study to elucidate the role of HSP90AB1 and EEF1A1 in the regulation of spermatogenesis and for discovery of new chemical structures that could serve as potential antispermatogenic male contraceptive agents.

MATERIALS AND METHODS

Preparation of Sertoli Cell-Enriched Cultures from 16-Day-Old Male Rats

Testes were collected from ten 16-day-old rats, washed, and decapsulated. Sertoli cells were obtained using the method described by Delfino and Walker [10]. All studies using animals were conducted under protocols approved by the University of Kansas Medical Center Institutional Animal Care and Use Committee as specified by federal guidelines.

Affinity Purification of Gamendazole-Binding Proteins

TM4 Sertoli cells and ID8 ovarian cancer cells. To ensure sufficient starting material for affinity purification, TM4 Sertoli cells [11], rather than primary Sertoli cells, were used to provide sufficient protein for affinity purification and comparable quantities of protein as testis cytosol. A nontumorigenic mouse cell line of Sertoli cell origin, TM4 cells retain FSH responsiveness. The TM4 cells were cultured in Dulbecco modified Eagle medium [DMEM]/F12 (50:50) with 5% horse serum and 2.5% fetal bovine serum to confluency on two 150-mm plates. After washing once with PBS, cells were lysed with 3 ml/plate of lysis buffer comprising 50 mM Tris-HCl (pH 7.4), 0.05 M NaCl, 0.001% NP-40, 5 mM EDTA, 50 mM NaF, 1 mM sodium orthovanadate, 1 mM sodium pyrophosphate, 10 mM benzamidine, 0.05 mg/ml of PMSF, 0.01 mg/ml of tosyl phenylalanyl chloromethylketone, 0.3 μg/ml aprotinin, and 0.3 μg/ml of soybean trypsin inhibitor. The cells in lysis buffer were scraped and transferred into a Dounce glass homogenizer and then homogenized with a tight pestle using 5–10 strokes to break the cells. After standing in ice for 30 min, the homogenate was centrifuged at 37 500 × *g* for 10 min at 4°C. The supernatant lysate was applied to a 2-ml avidin-agarose (tetramer form) column (preequilibrated with TD buffer [50 mM Tris-HCl, pH 7.4, and 0.001% NP-40]) to remove native biotinylated compounds and obtain a precleared lysate. The precleared cell lysate (2.7 ml) was incubated with 60 μM biotinylated gamendazole (BT-GMZ) (Fig. 1). A parallel control 2.7-ml aliquot of precleared lysate was incubated with 60 μM BT-GMZ plus a 10-fold molar excess of gamendazole. After incubation overnight at 4°C on a rocker platform, the samples were loaded on avidin-agarose columns preequilibrated with TD buffer and then washed with TD buffer until background was reached. The columns were sequentially eluted with 2.5 ml of TD buffer containing 0.6 mg/ml of gamendazole, then 250 mM NaCl, and finally, 600 mM NaCl. Each 2.5-ml eluate was collected and concentrated in a Centricon Y-10 (Millipore) for 2 h at 4°C at 5000 × *g* to a volume of 100–200 μl. Aliquots were removed for protein determination, and SDS-PAGE electrophoresis sample buffer was added. Electrophoresis was performed on a 5–20% gradient gel. Gels were fixed and silver-stained using the matrix-assisted laser desorption/ionization-time of flight (MALDI-TOF) compatible method described by Shevchenko et al. [12].

In a previous study [4], we noted that tumorigenic mouse ovarian surface epithelial (ID8) cells show growth inhibition in response to gamendazole. The ID8 cells were developed following a spontaneous transformation event in vitro [13, 14]. Injection of ID8 cells into the peritoneal cavity of athymic and syngeneic mice resulted in formation of ascites fluid and multiple tumor implants throughout the peritoneum. Histopathologic analysis of tumors revealed a highly malignant neoplasm containing carcinomatous and sarcomatous components.

The ID8 cells were cultured using standard procedures in complete medium (DMEM supplemented with 4% fetal bovine serum, 100 U/ml of penicillin, 100 μg/ml of streptomycin, 5 μg/ml of insulin, 5 μg/ml of transferrin, and 5 ng/ml of sodium selenite) at 37°C in a humidified atmosphere of 5% CO_2 and air. Cells were grown to near confluence in T75 flasks, washed twice with cold PBS, and placed in lysis buffer as described above, and the cytosols were prepared and subjected to affinity binding and electrophoresis as described above for the TM4 cells.

Rat testis. A testis cytosol from 60-day-old rats was prepared as follows: The detunicated testes from two rats (2.8 g total) were homogenized with a PowerGen homogenizer (Fisher) using three bursts of 10 sec each on ice in 6 ml of lysis buffer (see above), then sonicated using a Sonic Dismembranator (Fisher) for 5 sec at setting 5 on ice. The sample was placed on ice for 30 min and then centrifuged at 37 500 × *g* for 10 min at 4°C. The resulting cytosol was precleared through an avidin-agarose column as described above, then split into two 2.7-ml aliquots and incubated overnight at 4°C either with 60 μM BT-GMZ or with 60 μM BT-GMZ plus a 10-fold molar excess of gamendazole, then passed through an avidin-agarose column. Following methods similar to those described above, the columns were each first washed with buffer to achieve background, then eluted stepwise with 2.7 ml of 1.5 mM gamendazole, then 3.0 mM gamendazole, and finally, 600 mM NaCl to collect remaining proteins that were not eluted by gamendazole. Collected fractions were concentrated and run on 5–20% SDS-PAGE gels as described above. The testis SDS-PAGE gels were fixed and stained with the MALDI-TOF compatible Coomassie blue method described by Candiano et al. [15].

In Vitro Binding and Ultraviolet Cross-Linking of Gamendazole to Purified Bacterially Expressed Yeast HSP82 (HSP90) and Purified Yeast and Mammalian EEF1A1

Purified recombinant *Saccharomyces cerevisiae* HSP82 [16] (5 μg in 20 μl), *S. cerevisiae* TEF1 [17], TEF3 [17], HBS1 [18], or *Oryctolagus*

caniculus EEF1A1 were incubated with ultraviolet cross-linked BT-GMZ (UV-BT-GMZ) (Fig. 1) for 1 h at 4°C, then cross-linked for 20 min at 4°C with long-wave UV. Competition incubations were carried out with a 10-fold molar excess of gamendazole, lonidamine (LND), geldanamycin, and A4 (a novobiocin analogue [19]) before UV exposure. The protein was then run on a 7.5% SDS-PAGE gel, transferred to a polyvinylidene fluoride membrane, and blocked with 0.1% BSA in TTBS (50 mM Tris-HCl [pH 7.4], 50 mM NaCl, 5 mM EDTA, and 50 mM NaF). Next, the sheet was incubated with horse radish peroxidase-avidin, washed with TTBS, and incubated for 20 min with 3-amino-9-ethyl carbazole substrate for horse radish peroxidase (Zymed Invitrogen) to visualize the gamendazole-coupled protein.

Effect of Gamendazole on HSP90 Client Proteins in MCF-7 Cells and HSP90-Mediated Luciferase Refolding

Western blot analysis of HSP90-dependent client proteins was performed as described previously [20]. The ability of gamendazole to inhibit the HSP90-dependent refolding of thermally denatured firefly luciferase also was performed as described previously [21].

mant-GMPPNP and mant-GDP Binding Assay for TEF1

The binding affinity for 2′- or 3′-*O*-*N*-methylanthraniloyl (mant)-GDP and mant-GMPPNP to *S. cerevisiae* TEF1 in the presence and absence of gamendazole was determined by a fluorometric titration assay as described previously [22]. To examine whether gamendazole inhibits nucleotide binding of TEF1, 50 μM gamendazole was incubated with TEF1-binding buffer mix for 30 min at 25°C before adding fluorescently labeled nucleotides. Increased fluorescence of mant-nucleotides was observed by fluorescence resonance energy transfer, which excited tryptophans or tyrosines of TEF1 at 280 nm and used an emission wavelength of 440 nm for the mant moiety of the nucleotides. The protein and nucleotide complex-dependent fluorescence values were plotted against mant-GMPPNP or mant-GDP concentrations and fit to a hyperbolic curve to give the equilibrium dissociation constant (K_d).

Antiproliferative Effect of Gamendazole MCF-7 Cells

The antiproliferative effect of gamendazole was determined as described previously [21] using the CellTiter 96 AQueous Assay (Promega Corp., Madison, WI) as described by the manufacturer.

MALDI-TOF Mass Spectrometry

In-gel digestion and peptide mass fingerprint identification of proteins were performed in the Biochemical Research Service Laboratory at the University of Kansas. Electrophoretically separated protein bands were excised by hand and in-gel digested with modified sequencing-grade trypsin (Promega) as described previously [23]. The resulting peptide mixtures were desalted using ZipTips C_{18}, eluted on the sample plate with the matrix solution (10 mg/ml of α-cyano-carboxycinnamic acid in 50% acetonitrile/0.1% trifluoroacetic acid), and then analyzed on a Voyager-DE STR MALDI-TOF mass spectrometer (Applied Biosystems). The instrument was operated in positive reflector mode with the following parameters: accelerating voltage, 20 000 V; grid voltage, 75%; mirror voltage ratio, 1.12; guide wire, 0.01%; extraction delay time, 150 nsec; and laser power attenuator setting, 2200. Acquisition mass range was 900-2000 Da, with low mass gate set at 900, and a resolution of 7000–10 000 was achieved within that mass range. Internal mass calibration was performed using trypsin autolysis peaks (MH^+ 842.5021 and 2211.0968). Mascot peptide mass fingerprinting method was used to perform database searches with the UniProtKB/Swiss-Prot database. Peak list was created from the raw data using Data Explorer software (PerSeptive Biosystems, Inc., Framingham, MA). We applied peak deisotoping and a signal:noise ratio of 10 criteria. Search parameters were the following: mass tolerance, 50 ppm; one missed cleavage; and carboxymethylation of cysteine residues.

Immunofluorescence of HSP90AB1 and EEF1A1 in Gamendazole-Treated Primary Sertoli Cells

Primary Sertoli cells were plated on acid-washed poly-L-lysine coated glass cover slips in six-well plates. The cells were treated with 20 μM gamendazole at 37°C. Controls were treated with solvent carrier (final concentration, 0.2% dimethyl sulfoxide [DMSO]). After 24 h, the media were aspirated, and the cells were washed three times with 2 ml of TBS (10 mM Tris-HCl [pH 7.4] and 0.9% [w/v] NaCl). Next, the cells were fixed with 10% formaldehyde in TBS for 20 min at room temperature, washed three times for 10 min each time with TBS, then permeabilized with 1% NP-40 in TBS (TBS-NP-40) for 15 min. The cells were then washed with TBS-NP-40 and blocked for 1 h at room temperature with 10% goat serum in TBS-NP-40. After rinsing with TBS, the cells were incubated for 1 h at 37°C with primary antibody, either a 1:1000 dilution of mouse monoclonal immunoglobulin G anti-EEF1A1 (05-235; Upstate) or a 1:1000 dilution of mouse monoclonal immunoglobulin M anti-HSP90AB1 (SPA-843; StressGen Biotechnologies) in 2% goat serum and 0.1% BSA in TBS-NP-40. After three washes with TBS-NP-40, the cells were incubated in the dark for 1 h at room temperature with tetramethyl rhodamine isothiocyanate-tagged secondary antibody (in the same buffer as primary antibody) as follows: For EEF1A1, 1:200 goat anti-mouse immunoglobulin G (115-025-003; Jackson Immunologicals); for HSP90AB1, 1:200 goat anti-mouse immunoglobulin M (115-025-020; Jackson Immunologicals). After the final three washes with TBS-NP-40 (10 min each), cover slips were mounted with Vectashield Hardset mounting media (Vector Laboratories) for fluorescence.

Gene Microarray Analysis of Testis from Rats Treated with Gamendazole Versus LND

In all treatment groups, animals were dosed via i.p. injection with a DMSO vehicle. The treatment groups were as follows: control (DMSO), 6 mg/kg of gamendazole, and 25 of mg/kg of LND. Animals were killed at 4, 12, and 24 h postinjection, including one 0-h control animal. The testes of each animal were collected and weighed. The right testes were placed in TRIzol reagent (Invitrogen), homogenized, and flash-frozen. The left testes were placed in 10% neutral buffered formalin (Sigma) for histological evaluation. The left testes were processed and embedded in paraffin following a 24-h incubation in 10% neutral buffered formalin. The RNA isolated from the right testes using TRIzol Reagent with Phase Lock Gel-Heavy protocol (5 Prime, Inc., Gaithersburg, MD) was then sent to the Microarray Core at the University of Kansas Medical Center and analyzed using Affymetrix microarray chips with probe array type Rat 230.2 (summarized in *Supplementary Data* online at www.biolreprod.org). The resulting data were analyzed using Affymetrix and GeneSpring software. The outstanding genes affected were confirmed using RT-PCR and Western blot analysis on primary cell lines.

Analysis of Microarray Data

The microarray experiment design included three chips for each time point (4, 12, and 24 h), with an additional control chip for the starting point (0 h). All time points were represented by a control and two treatments (LND and gamendazole). The initial data captured by Affymetrix software resulted in a single raw value for each probe set based on the mean of the differences between the intensity of hybridization for a perfect match and the mismatch features for a specific transcript (online GeneChip Expression Analysis; http://www.affymetrix.com/support/technical/manual/expression_manual.affx).

Expression analysis data were exported via Data Transfer Tool into the data library by the Affymetrix GeneChip Operating Software. We used the Data Mining Tool component to process the data quality control and subsets of expressed probes. A total set of 31 099 probes for this particular genome (Rat 230_2.0) was divided into present, marginal, and absent subsets based on the detection *P* value. When the detection *P* value (Student *t*-test) is less than 5% (i.e., <0.05), then the detection is designated as present, because the particular probe is detected with more than 95% significance. When the detection *P* value is between 5% and 6.5%, the detection interpretation is designated as marginal, lowering the significance level to under 95%. If the detection value exceeds 6.5%, the probes are designated as absent. Present and absent probes across all chips in this experiment showed very similar distribution (≈50%), whereas the marginal probes represented only small fraction of probes ($<1.7\%$).

To evaluate the upregulated genes, only present probes in the treatment versus all probes in the control were used, whereas for downregulated genes, present probes in control were used versus all probes in the treatment set. We created sets of upregulated/downregulated genes for combinations in all time points and both treatments versus control data and between individual treatments with the fold-change exceeding 2.0-fold. GeneChip data from Affymetrix were then transferred into text file inputs for the GeneSpring 7.1 (Agilent Technologies) software to obtain the full updated gene annotation.

Data were sorted by the fold-change and presented in table formats with probe, fold-change, treatment and control characteristic (signal, detection, and detection *P* value), and full gene annotation. The complete gene microarray data set is available at http://www.ncbi.nlm.nih.gov/geo/ in series record GSE8485.

RT-PCR of Il1a in Primary Sertoli Cells Treated with Gamendazole

Rat primary Sertoli cells were obtained as described above, plated on 14 six-well plates, and incubated in medium containing serum-free supplemented

DMEM/F-12 for 72 h at 33°C. The medium was removed and replaced with fresh medium containing three varying concentrations of gamendazole (100 nM) dissolved in DMSO (final concentration in medium, 0.1%). The cells were returned to 37°C and incubated for 0, 30, 60, 120, or 240 min. Following the appropriate drug incubation period, RNA samples were extracted from the primary Sertoli cells with TRIzol reagent according to the manufacturer's instructions. One microliter from each RNA sample was diluted in 99 μl of RNase-free water and subjected to UV analysis using an Eppendorf Biophotometer. These values were used to ensure equal amounts of RNA starting material for cDNA synthesis performed on a 2720 Thermal Cycler (Applied Biosystems). The RNA mixture for cDNA synthesis consisted of 1 μg of RNA (calculated from UV analysis) and 1 μl of Oligo-dT and was brought up to a total volume of 11 or 12 μl with RNase-free H_2O. The mixture was heated for 10 min at 70°C and then quickly chilled on ice. Four microliters of cocktail, containing 2 μl of reaction first-strand buffer, 0.1 M dithiothreitol, 0.5 μl of reaction RNasin, and 25 mM dNTPs, were added, and the mixture was incubated at 42°C for 2 min. Finally, 1 μl of SuperScript II was added to the positive controls. Aliquots (10 μl) of all samples were separated on a 1% agarose gel containing ethidium bromide. Each gel was run for 20 min at 120 V and photographed under UV light. PCR analysis required the design of *Il1a* nucleotide primers. This was accomplished with DS Gene (Accelrys, Inc., San Diego, CA), a nucleic acid and protein sequence analysis software program. The gene-specific primers were screened for hairpins and dimers using NetPrimer (provided online by Premier Biosoft International http://www.premierbiosoft.com/). Integrated DNA Technologies, Inc., was used for the actual synthesis. The upstream primer (5′ GCC ATT GAC CAT CTG TCT CTG 3′) corresponds to positions 131–157 in the published sequence [24]. The downstream primer (5′ GCT GAG TAT TTG AGA CTT TGA GAG 3′) corresponds to positions 641–618. The primers were deliberately chosen so that they would encompass several exons to avoid confusion with any amplified genomic *Il1a* DNA [25]. The PCR was performed in a reaction volume of 25 μl in the presence of 0.26 μM of the *Il1a* nucleotide primers, 0.1 mM dNTP, 1 mM $MgCl_2$, and Taq polymerase. The steps in the PCR reaction included time delay (94°C for 5 min), step-cycle (96°C for 1 min, 51°C for 30 sec, and 72°C for 30 sec) for a total of 35 cycles, a 5-min time delay at 72°C, and finally, a soak file at 4°C for at least 5 min. Aliquots (10 μl) of all samples were separated on a 1% agarose gel containing ethidium bromide. The gel was run for 20 min at 120 V and digitally imaged using an Alpha Innotech Digital Imager.

RESULTS

Affinity Binding of HSP90AB1 and EEF1A1 by Gamendazole in Testis and Sertoli Cell Cytosols

Our previous study demonstrated that gamendazole elicits a dramatic decrease in circulating inhibin B levels in vivo and that primary cultures of Sertoli cells show a decline in inhibin production in vitro after gamendazole treatment, with a median inhibitory concentration (IC_{50}) of 6.8×10^{-10} M [4]. This suggests that testis, and Sertoli cells in particular, contain a target, or targets, with high affinity for the compound. To test this hypothesis, BT-GMZ (Fig. 1) was employed as a ligand in avidin-affinity chromatography (Fig. 2) followed by MALDI-TOF mass spectrometry to identify proteins contained in the excised affinity bands. As noted below, we focused attention on bands that were consistently pulled out of the cytosol from all tissues or cells that were studied previously and found to be affected by gamendazole treatment: Sertoli cells (TM4 cells) (Fig. 2A), rat testis (Fig. 2B), and ID8 ovarian cancer cells (Fig. 2C) [4].

Protein bands at 90 and 53 kDa were consistently observed in the gamendazole and subsequent high-salt eluate from all three cytosol sources. Furthermore, each 90- and 53-kDa band, respectively, exhibited the same gamendazole and salt elution profile as well as comparable reduction in signal by excess gamendazole competition from all three cytosol sources. The top-ranked protein matches for the 90-kDa band from TM4 cells (Fig. 3) and testis (Fig. 4) were both HSP90AB1 (molecular weight [MW], 83 229, P34058; scores of 37 and 78, respectively). Although the score for the testis band was below the significance level (score, 50), provided by Mascot default at 5%, additional evidence for the successful identification was that the proteins were excised from the 90-kDa gel bands. In addition, seven peptide matches, comprising 14% coverage of the entire HSP90AB1 sequence, were made with the TM4 90-kDa band, and 12 peptides, comprising 18% of the entire sequence, were matched with the testis 90-kDa band. The top-ranked protein matches for the 53-kDa band from TM4 cells (Fig. 5) and testis (Fig. 6) were both EEF1A1–1 (MW, 50 082, P62630; scores of 54 and 36, respectively).

Confidence in the identification of this protein comes from the expected MW of approximately 50 000 as determined by gel electrophoresis. In addition, four peptide matches, comprising 14% coverage of the entire sequence, were made with the TM4 53-kDa band, and seven peptides, comprising 17% of the entire EEF1A1 sequence, were matched for the testis 53-kDa band.

It should be noted that the MALDI-TOF mass spectra obtained from the pull-downs from TM4 and testis cytosols (see below) were what one would expect from low-abundance gel bands dominated by trypsin autolysis and the usual keratin contaminants. Clear data, however, indicate that HSP90AB1 and EEF1A1 were in the indicated spots. In all cases, multiple matching peptides were detected.

The affinity purification and elution profiles for the HSP90AB1- and EEF1A1-containing bands were consistent with gamendazole binding directly to these proteins or to a protein complex containing these proteins. First, in the eluates before the high-salt bumps, the bands containing these proteins bound to the avidin column in a gamendazole-dependent manner. Comparison of the gamendazole-eluted protein profiles from the cytosols initially incubated without and with excess gamendazole revealed the 90-kDa protein was selectively eluted from the column by gamendazole (Fig. 2A, lane 3) but was absent in the gamendazole eluate that was preblocked by excess gamendazole (Fig. 2A, lane 4). In the subsequent NaCl eluates, a 90-kDa band also was present but showed gamendazole-dependent competition binding to the column (Fig. 2A, lanes 6 and 8). The identity of this band is not known. A band at 53-kDa also was observed in the high-salt eluates but was absent in the gamendazole preblocked eluates (Fig. 2A, lanes 5–8). This band also was identified as EEF1A1 by MALDI-TOF mass spectrometry and by sequencing and resulting match of 7 of 36 resulting peptides, with a minimum of 17% sequence coverage (Fig. 6).

A similar affinity purification experiment using cytosol from 60-day-old rat testis also revealed HSP90AB1 and EEF1A1 in the gamendazole-binding proteins (Fig. 2B). Comparison of the gamendazole-eluted protein profiles from the testis cytosols incubated without and with excess gamendazole revealed a 90-kDa protein that was eluted from the column by gamendazole (Fig. 2B, lanes 3 and 4) but was absent in the gamendazole eluate that was preblocked by excess gamendazole (Fig. 2B, lanes 6 and 7). Western blot analysis of the eluted samples confirmed the presence of HSP90 in a elution pattern that matched the 90-kDa Coomassie-stained band. A Western blot signal corresponding to a 90-kDa band HSP90 present in the starting precleared cytosols (Fig. 2B, lanes 1 and 2) was eluted by 1.5 and 3.0 mM gamendazole (Fig. 2B, lanes 3–4) but was absent in the eluates from the cytosol preincubated with a 10-fold excess of gamendazole (Fig. 2B, lanes 3 and 4). In addition, an HSP90 Western blot signal was observed that corresponds to the 90-kDa Coomassie-stained band in the salt eluate (Fig. 2B, lane 7) but was absent in the excess gamendazole-binding control (Fig. 2B, lane 8). These results demonstrate that the 90-kDa band in the pre-high-salt eluates contained HSP90 and that the

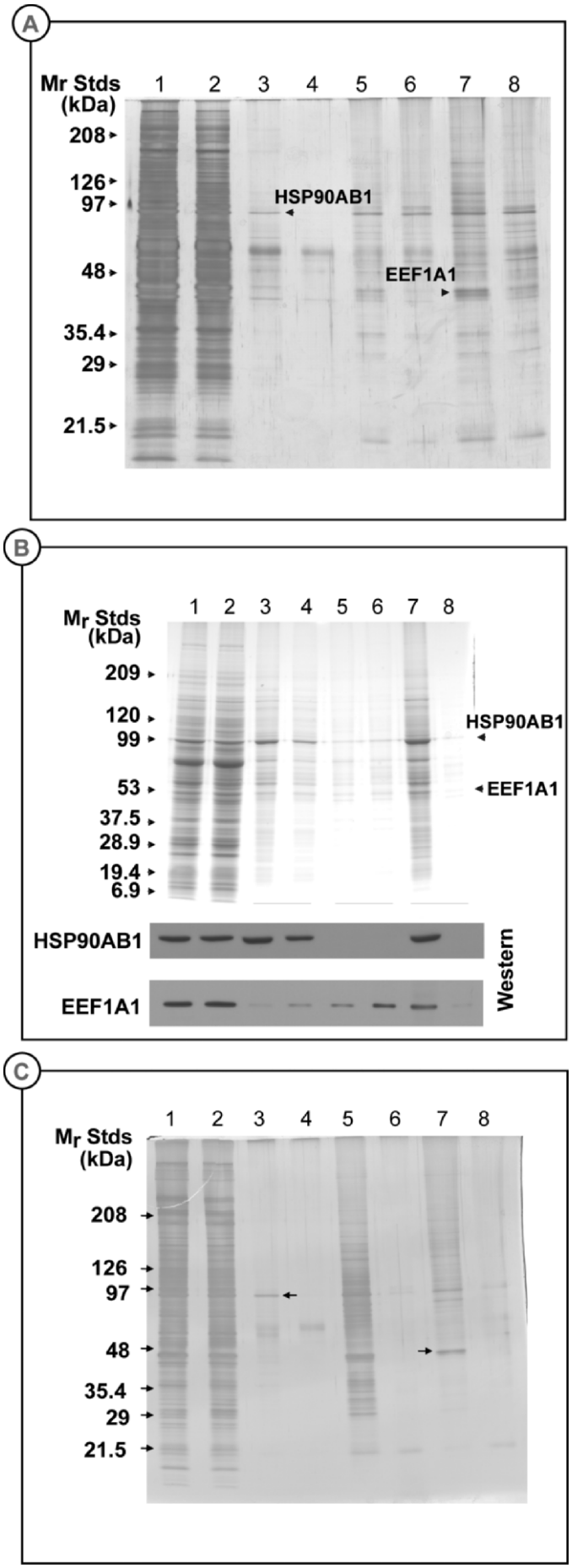

binding of the protein(s) in this band and its elution were dependent on gamendazole binding either directly to the 90-kDa band itself or to a binding partner. MALDI-TOF analysis of the 90-kDa bands confirmed that this band contained HSP90AB1 (Fig. 3). As observed with TM4 cells, a component of proteins at 90 kDa is resistant to gamendazole-dependent binding and elution and requires high salt to be removed from the column (Fig. 2B, lane 7). The Western blot data suggest that HSP90 was present in the 600 mM salt eluate (Fig. 2B, lane 7) and that its binding to the column was still gamendazole-dependent (Fig. 2B, lane 8). Thus, it may have required higher levels of gamendazole or longer exposure to competing compound to elute from the column before application of the high salt.

A band containing EEF1A1 in the high-salt eluate that was blocked by excess gamendazole was confirmed by Western blot analysis. This analysis also revealed EEF1A1 in the gamendazole preblocked sample that eluted from the column with higher concentrations of gamendazole (3.0 mM). The elution pattern for the EEF1A1 signal suggests that the gamendazole-dependent binding to the column was tighter than that for HSP90, because the EEF1A1 band was eluted not with 1.5 mM gamendazole but with higher concentrations and mainly in the high-salt eluate from the column after gamendazole had already been applied to the column. The presence of a Western blot signal for EEF1A1 in the 6 mM gamendazole eluate from the excess gamendazole preincubated control could be explained by a high-affinity binding site in EEF1A1 combined with the presence of large quantities of EEF1A1 in the cytosol.

Both HSP90 and EEF1A1 have been proposed as drug targets for anticancer therapeutic agents [26, 27]. Thus, we examined the possibility that gamendazole could bind to the same protein targets in a cancer cell. We have already shown that ID8 cells show growth inhibition when cultured in the presence of gamendazole [4]. As presented in Figure 2C, two very prominent and clean protein bands were eluted from the

FIG. 2. **A**) TM4 Sertoli cell cytosol protein affinity binding using biotinylated gamendazole (BT-GMZ): Lanes 1 and 2: silver-stained starting cytosol and precleared avidin-agarose-treated cytosol, respectively; lanes 3 and 4: gamendazole eluates obtained from cytosols incubated with BT-GMZ in the absence (lane 3) and the presence (lane 4) of a 10-fold excess of gamendazole; lanes 5 and 7: 250 and 600 mM NaCl eluates, respectively, from the column to which cytosol incubated with BT-GMZ alone was applied; lanes 6 and 8: 250 and 600 mM NaCl eluates, respectively, from the column to which cytosol incubated with BT-GMZ plus excess gamendazole was applied. The arrow in lane 3 indicates the band identified by MALDI-TOF mass spectrometry as HSP90AB1 (see Fig. 3); the arrow in lane 7 indicates the band that was identified by MALDI-TOF mass spectrometry as EEF1A1 (see Fig. 4). **B**) Rat testis cytosol protein affinity binding using BT-GMA: Coomassie-stained starting cytosol and precleared avidin-agarose treated cytosol are shown in lanes 1 and 2, respectively. The columns were eluted stepwise with 1.5 mM gamendazole (lanes 3 and 4), then with 3.0 mM gamendazole (lanes 5 and 6), and then with 600 mM NaCl (lanes 7 and 8); the first lane in each pair represents the eluate from the cytosol that was incubated with BT-GMZ and the second lane the eluate from the cytosol incubated with BT-GMZ plus excess gamendazole. The arrow at 90 kDa indicates the band in lane 3 that was identified by MALDI-TOF mass spectrometry as HSP90AB1 (see Fig. 5). The arrow at 53 kDa indicates the band in lane 7 that was identified by MALDI-TOF mass spectrometry as EEF1A1 (see Fig. 6). The bottom two images depict Western blots of HSP90AB1 and EEF1A1 showing the corresponding regions of the gel indicated by the arrows at HSP90AB1 and EEF1A1, respectively. **C**) ID8 ovarian cancer cell cytosol protein affinity binding using BT-GMZ. Lanes represent treatments identical to those in **A**. Arrows in lanes 3 and 7 indicate the bands corresponding to positions of HSP90AB1 and EEF1A1, respectively.

Fig. 3

Match to: **P34058|HS90B_RAT** Score: **37** Expect: **1.2**
Heat shock protein HSP 90-beta - Rattus norvegicus (Rat)

Nominal mass (M_r): **83229**; Calculated pI value: **4.97**
NCBI BLAST search of P34058|HS90B_RAT against nr

Taxonomy: Rattus norvegicus

Matched peptides shown in **Bold Red**

```
    1 MPEEVHHGEE EVETFAFQAE IAQLMSLIIN TFYSNKEIFL RELISNASDA
   51 LDKIRYESLT DPSKLDSGKE LKIDIIPNPQ ERTLTLVDTG IGMTKADLIN
  101 NLGTIAKSGT KAFMEALQAG ADISMIGQFG VGFYSAYLVA EKVVVITKHN
  151 DDEQYAWESS AGGSFTVRAD HGEPIGRGTK VILHLKEDQT EYLEERRVKE
  201 VVKKHSQFIG YPITLYLEKE REKEISDDEA EEEKGEKEEE DKEDEEKPKI
  251 EDVGSDEEDD SGKDKKKKTK KIKEKYIDQE ELNKTKPIWT RNPDDITQEE
  301 YGEFYKSLTN DWEDHLAVKH FSVEGQLEFR ALLFIPRRAP FDLFENKKKK
  351 NNIKLYVRRV FIMDSCDELI PEYLNFIRGV VDSEDLPLNI SREMLQQSKI
  401 LKVIRKNIVK KCLELFSELA EDKENYKKFY EAFSKNLKLG IHEDSTNRRR
  451 LSELLRYHTS QSGDEMTSLS EYVSRMKETQ KSIYYITGES KEQVANSAFV
  501 ERVRKRGFEV VYMTEPIDEY CVQQLKEFDG KSLVSVTKEG LELPEDEEEK
  551 KKMEESKAKF ENLCKLMKEI LDKKVEKVTI SNRLVSSPCC IVTSTYGWTA
  601 NMERIMKAQA LRDNSTMGYM MAKKHLEINP DHPIVETLRQ KAEADKNDKA
  651 VKDLVVLLFE TALLSSGFSL EDPQTHSNRI YRMIKLGLGI DEDEVTAEEP
  701 SAAVPDEIPP LEGDEDASRM EEVD
```

Start - End	Observed	Mr(expt)	Mr(calc)	Delta	Miss	Sequence
331 - 337	829.5346	828.5273	828.5221	0.0052	0	R.ALLFIPR.R
169 - 177	951.4785	950.4712	950.4570	0.0143	0	R.ADHGEPIGR.G
338 - 347	1236.6400	1235.6327	1235.6298	0.0029	1	R.RAFFDLFENK.K
320 - 330	1348.6788	1347.6716	1347.6571	0.0145	0	K.HFSVEGQLEFR.A
70 - 82	1564.8728	1563.8655	1563.8620	0.0035	1	K.ELKIDIIPNPQER.T
625 - 639	1782.9200	1781.9128	1781.9424	-0.0296	0	K.KLEINPDHPIVETLR.Q
624 - 639	1911.0147	1910.0074	1910.0374	-0.0299	1	K.KKLEINPDHPIVETLR.Q

Fig. 4

Match to: **P62630|EF1A1_RAT** Score: **54** Expect: **0.024**
Elongation factor 1-alpha 1 - Rattus norvegicus (Rat)

Nominal mass (M_r): **50082**; Calculated pI value: **9.10**
NCBI BLAST search of P62630|EF1A1_RAT against nr

Taxonomy: Rattus norvegicus

Matched peptides shown in **Bold Red**

```
    1 MGKEKTHINI VVIGHVDSGK STTTGHLIYK CGGIDKRTIE KFEKEAAEMG
   51 KGSFKYAWVL DKLKAERERG ITIDISLWKF ETSKYYVTII DAPGHRDFIK
  101 NMITGTSQAD CAVLIVAAGV GEFEAGISKN GQTREHALLA YTLGVKQLIV
  151 GVNKMDSTEP PYSQKRYEEI VKEVSTYIKK IGYNPDTVAF VPISGWNGDN
  201 MLEPSANMPW FKGWKVTRKD GSASGTTLLE ALDCILPPTR PTDKPLRLPL
  251 QDVYKIGGIG TVPVGRVETG VLKPGMVVTF APVNVTTEVK SVEMHHEALS
  301 EALPGDNVGF NVKNVSVKDV RRGNVAGDSK NDPPMEAAGF TAQVIILNHP
  351 GQISAGYAPV LDCHTAHIAC KFAELKEKID RRSGKKLEDG PKFLKSGDAA
  401 IVDMVPGKPM CVESFSDYPP LGRFAVRDMR QTVAVGVIKA VDKKAAGAGK
  451 VTKSAQKAQK AK
```

Start - End	Observed	Mr(expt)	Mr(calc)	Delta	Miss	Sequence
256 - 266	1025.6312	1024.6240	1024.6029	0.0211	0	K.IGGIGTVPVGR.V
135 - 146	1314.7368	1313.7295	1313.7343	-0.0047	0	K.EHALLAYTLGVK.Q
85 - 96	1404.7212	1403.7139	1403.7197	-0.0058	0	K.YYVTIIDAPGHR.D
6 - 20	1588.8999	1587.8926	1587.8732	0.0194	0	K.THINIVVIGHVDSGK.S
38 - 51	1610.8040	1609.7967	1609.8021	-0.0054	2	R.TIEKFEKEAAEMGK.G
21 - 37	1907.9786	1906.9714	1906.9570	0.0143	2	K.STTTGHLIYKCGGIDKR.T Carboxymethyl (C)
267 - 290	2515.2954	2514.2881	2514.3766	-0.0885	0	R.VETGVLKPGMVVTFAPVNVTTEVK.S

Fig. 5

Match to: **P34058|HS90B_RAT** Score: **78** Expect: **8.9e-005**
Heat shock protein HSP 90-beta - Rattus norvegicus (Rat)

Nominal mass (M_r): **83229**; Calculated pI value: **4.97**
NCBI BLAST search of P34058|HS90B_RAT against nr

Taxonomy: Rattus norvegicus

Matched peptides shown in **Bold Red**

```
    1 MPEEVHHGEE EVETFAFQAE IAQLMSLIIN TFYSNKEIFL RELISNASDA
   51 LDKIRYESLT DPSKLDSGKE LKIDIIPNPQ ERTLTLVDTG IGMTKADLIN
  101 NLGTIAKSGT KAFMEALQAG ADISMIGQFG VGFYSAYLVA EKVVVITKHN
  151 DDEQYAWESS AGGSFTVRAD HGEPIGRGTK VILHLKEDQT EYLEERRVKE
  201 VVKKHSQFIG YPITLYLEKE REKEISDDEA EEEKGEKEEE DKEDEEKPKI
  251 EDVGSDEEDD SGKDKKKKTK KIKEKYIDQE ELNKTKPIWT RNPDDITQEE
  301 YGEFYKSLTN DWEDHLAVKH FSVEGQLEFR ALLFIPRRAP FDLFENKKKK
  351 NNIKLYVRRV FIMDSCDELI PEYLNFIRGV VDSEDLPLNI SREMLQQSKI
  401 LKVIRKNIVK KCLELFSELA EDKENYKKFY EAFSKNLKLG IHEDSTNRRR
  451 LSELLRYHTS QSGDEMTSLS EYVSRMKETQ KSIYYITGES KEQVANSAFV
  501 ERVRKRGFEV VYMTEPIDEY CVQQLKEFDG KSLVSVTKEG LELPEDEEEK
  551 KKMEESKAKF ENLCKLMKEI LDKKVEKVTI SNRLVSSPCC IVTSTYGWTA
  601 NMERIMKAQA LRDNSTMGYM MAKKHLEINP DHPIVETLRQ KAEADKNDKA
  651 VKDLVVLLFE TALLSSGFSL EDPQTHSNRI YRMIKLGLGI DEDEVTAEEP
  701 SAAVPDEIPP LEGDEDASRM EEVD
```

Start - End	Observed	Mr(expt)	Mr(calc)	Delta	Miss	Sequence
331 - 337	829.5129	828.5056	828.5221	-0.0165	0	R.ALLFIPR.R
285 - 291	901.5076	900.5003	900.5181	-0.0178	0	K.TKFIWTR.N
169 - 177	951.4491	950.4418	950.4570	-0.0151	0	R.ADHGEPIGR.G
575 - 583	1045.5754	1044.5682	1044.5927	-0.0245	1	K.VEKVTISNR.L
73 - 82	1194.6444	1193.6371	1193.6404	-0.0033	0	K.IDIIPNPQER.T
338 - 347	1236.6484	1235.6412	1235.6298	0.0113	1	R.RAFFDLFENK.K
320 - 330	1348.6726	1347.6653	1347.6571	0.0082	0	K.HFSVEGQLEFR.A
379 - 392	1513.8073	1512.8000	1512.7783	0.0216	0	R.GVVDSEDLPLNISR.E
42 - 55	1544.8164	1543.8091	1543.8205	-0.0114	1	R.ELISNASDALDKIR.Y
70 - 82	1564.8555	1563.8482	1563.8620	-0.0138	1	K.ELKIDIIPNPQER.T
625 - 639	1782.9346	1781.9273	1781.9424	-0.0151	0	K.KLEINPDHPIVETLR.Q
624 - 639	1911.0322	1910.0250	1910.0374	-0.0124	1	K.KKLEINPDHPIVETLR.Q
181 - 196	2014.9954	2013.9881	2014.0371	-0.0490	1	K.VILNLKEDQTEYLEER.R

Fig. 6

Match to: **P62630|EF1A1_RAT** Score: **36** Expect: **1.5**
Elongation factor 1-alpha 1 - Rattus norvegicus (Rat)

Nominal mass (M_r): **50082**; Calculated pI value: **9.10**
NCBI BLAST search of P62630|EF1A1_RAT against nr

Taxonomy: Rattus norvegicus

Matched peptides shown in **Bold Red**

```
    1 MGKEKTHINI VVIGHVDSGK STTTGHLIYK CGGIDKRTIE KFEKEAAEMG
   51 KGSFKYAWVL DKLKAERERG ITIDISLWKF ETSKYYVTII DAPGHRDFIK
  101 NMITGTSQAD CAVLIVAAGV GEFEAGISKN GQTREHALLA YTLGVKQLIV
  151 GVNKMDSTEP PYSQKRYEEI VKEVSTYIKK IGYNPDTVAF VPISGWNGDN
  201 MLEPSANMPW FKGWKVTRKD GSASGTTLLE ALDCILPPTR PTDKPLRLPL
  251 QDVYKIGGIG TVPVGRVETG VLKPGMVVTF APVNVTTEVK SVEMHHEALS
  301 EALPGDNVGF NVKNVSVKDV RRGNVAGDSK NDPPMEAAGF TAQVIILNHP
  351 GQISAGYAPV LDCHTAHIAC KFAELKEKID RRSGKKLEDG PKFLKSGDAA
  401 IVDMVPGKPM CVESFSDYPP LGRFAVRDMR QTVAVGVIKA VDKKAAGAGK
  451 VTKSAQKAQK AK
```

Start - End	Observed	Mr(expt)	Mr(calc)	Delta	Miss	Sequence
372 - 378	864.4830	863.4757	863.4752	0.0005	1	K.FAELKEK.I
147 - 154	870.5349	869.5276	869.5334	-0.0058	0	K.QLIVGVNK.M
248 - 255	975.5384	974.5311	974.5437	-0.0125	0	R.LPLQDVYK.I
256 - 266	1025.6122	1024.6049	1024.6029	0.0020	0	K.IGGIGTVPVGR.V
85 - 96	1404.7209	1403.7137	1403.7197	-0.0060	0	K.YYVTIIDAPGHR.D

PLATE I. Figures 3, 4, 5, and 6.

FIG. 3. MALDI-TOF peptide sequence match and positions in HSP90AB1 for gamendazole affinity-purified 90-kDa band from TM4 cytosol. Mascot peptide mass fingerprinting method was used to perform database searches using the UniProtKB/Swiss-Prot database. The complete amino acid sequence of the highest score match (HSP90AB1) is shown, with the position of the matched peptides indicated in red. The amino acid sequence of each of the matched peptides is listed at the bottom in order of peptide length. See *Materials and Methods* for additional experimental details.

FIG. 4. MALDI-TOF peptide sequence match and positions in EEF1A1 for gamendazole affinity-purified 53-kDa band from TM4 cytosol. Mascot peptide mass fingerprinting method was used to perform database searches using the UniProtKB/Swiss-Prot database. The complete amino acid sequence of the highest score match (EEF1A1) is shown, with the position of the matched peptides indicated in red. The amino acid sequence of each of the matched peptides is listed at the bottom in order of peptide length. See *Materials and Methods* for additional experimental details.

FIG. 5. MALDI-TOF peptide sequence match and positions in HSP90AB1 for gamendazole affinity-purified 90-kDa band from rat testis cell cytosol. See Figure 3 and *Materials and Methods* for experimental details.

FIG. 6. MALDI-TOF peptide sequence match and positions in EEF1A1 for gamendazole affinity-purified 53-kDa band from rat testis cell cytosol. See Figure 4 and *Materials and Methods* for experimental details.

column and behaved identically to HSP90AB1 and EEF1A1, respectively, with regard to elution, relative molecular weight, and competition of binding by excess gamendazole.

Direct Binding of Gamendazole by Purified HSP82 and EEF1A1

The affinity purification of HSP90AB1 and EEF1A1 from testis and Sertoli cell cytosols using BT-GMZ suggests either direct or indirect binding of HSP90 and EEF1A1 by gamendazole. Direct binding of HSP90 was confirmed using purified recombinant *S. cerevisiae* HSP82 (homologue to HSP90AB1) and UV-BT-GMZ (Fig. 7A). In the presence of a fixed amount of HSP82, as the concentration of UV-BT-GMZ increased, the signal of bound compound increased (Fig. 7A, top lane). The signal for UV-BT-GMZ was reduced in the presence of competing gamendazole, indicating specific gamendazole binding (Fig. 7A, middle lane). Competition of gamendazole binding by LND was not achieved until 10 mM LND and above (Fig. 7A, bottom lane). This suggests that binding of HSP82 by gamendazole is much tighter than that by LND. This conclusion is supported by attempts to affinity purify targets from testis using biotinylated UV cross-linking LND. No LND-specific binding could be achieved following similar procedures (data not shown).

The direct binding of gamendazole to HSP82 was explored further by testing whether known inhibitors of HSP90 could compete for UV-BT-GMZ binding (Fig. 7B). The HSP90 family members contain an N-terminal and a C-terminal ATP-binding site. Two known inhibitors of HSP90 function are geldanamycin, an inhibitor of the N-terminal ATP site, and novobiocin, an inhibitor of the C-terminal ATP site [28, 29].

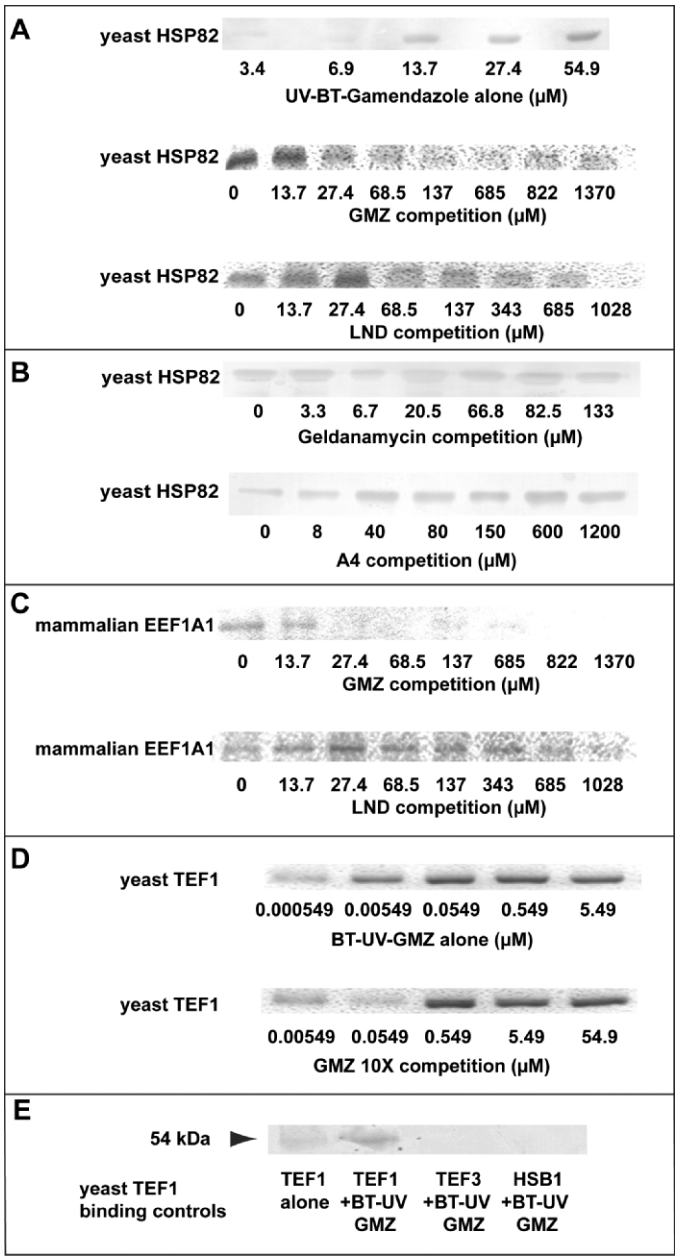

FIG. 7. **A**) Direct binding of UV-BT-GMZ to purified *S. cerevisae* HSP82 and competition by gamendazole and LND. **B**) Competition binding of 13.7 μM UV-BT-GMZ with the HSP90 inhibitors geldanamycin and KU-1 to purified yeast HSP82. **C**) Competetive binding of 13.7 μM UV-BT-GMZ to purified *O. caniculus* EEF1A1 by gamendazole and LND. **D**) Direct binding of UV-BT-GMZ to purified *S. cerevisiae* TEF1 and competetive binding by gamendazole. **E**) Direct binding of UV-BT-GMZ to purified *S. cerevisiae* TEF1 and absence of binding to the control proteins TEF3 and HSB1.

We recently synthesized A4, an analogue of novobiocin, with a low-micromolar affinity for HSP90 [19], as opposed to the low-millimolar affinity of novobiocin for HSP90. Neither geldanamycin nor A4 competed for binding of UV-BT-GMZ by HSP82. This suggests that either gamendazole binds to HSP90 with much higher affinity than either geldanamycin or A4 or that gamendazole binds to a different site on HSP90 than the other compounds do. Studies to elucidate the gamendazole-binding site are currently in progress, and results from such studies will be reported in due course.

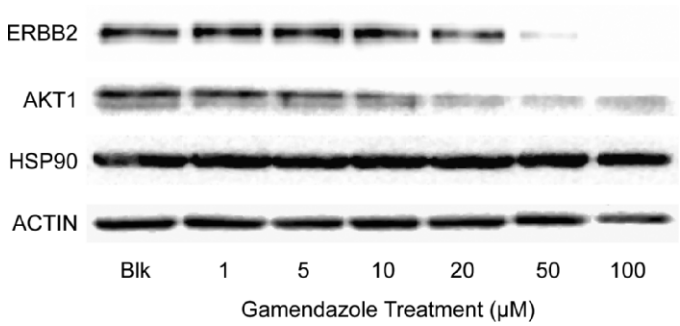

FIG. 8. Western blot analysis of ERBB2, AKT1, HSP90, and actin in MCF-7 cells treated with gamendazole. All concentrations are reported in micromoles, and geldanamycin (500 nM), a known HSP90 inhibitor, was used as a positive control.

Direct binding and competition of gamendazole binding to purified *O. caniculus* EEF1A1 (Fig. 7C) and its homologue *S. cerevisiae* TEF1 (Fig. 7D) also was confirmed following similar procedures. In the presence of fixed amounts of TEF1, concentrations of UV-BT-GMZ alone at 54.9 nM and above showed no additional increase in signal, indicating saturation of the protein at these concentrations (Fig. 7D, upper lane). At the subsaturating concentrations of UV-BT-GMZ, a 10-fold excess of gamendazole competed binding, as indicated by the lower binding signal (Fig. 7D, lower lane). To control for the specificity of cross-linking to TEF1, reactions with UV-BT-GMZ also were performed with two other purified yeast nucleotide binding proteins: HBS1, a GTP-binding protein, and TEF3, an ATP-binding protein. At equal concentrations and ratios to UV-BT-GMZ as used for TEF1, no cross-linking to either protein could be observed (Fig. 7E).

Gamendazole Affects HSP90 Client Proteins In Vitro

The affinity purification results and in vitro HSP90-binding studies described above demonstrate that gamendazole binds directly to HSP90. To determine whether gamendazole produces a functional change in HSP90, we undertook a series of cell-based and in vitro experiments that have been used previously to measure distinct functional changes in HSP90 resulting from direct drug binding [21, 26, 30]. In the presence of inhibitors, the substrate-bound HSP90 heteroprotein complex becomes destabilized, and the client protein becomes a target for ubiquitin-proteasomal degradation. Thereby, disruption of HSP90-mediated protein folding processes result in the degradation of HSP90-dependent client proteins [26]. We decided to test the MCF-7 breast cancer cell line, in which numerous HSP90 inhibitors have been analyzed, to provide the most appropriate confirmation of HSP90 inhibitory activity [30].

To determine whether gamendazole affects the HSP90-mediated protein folding process, Western blot analyses of MCF-7 breast cancer cell lysates were performed (Fig. 8). Both ERBB2 (HER2) and AKT1 are known HSP90-dependent client proteins that require HSP90 for conformational maturation [30]. Gamendazole caused the degradation of these two HSP90 substrates in a dose-dependant manner (Fig. 8). Actin is not a substrate for the HSP90 protein folding process, and in the presence of gamendazole, levels of actin remained the same, supporting the hypothesis that the effects of gamendazole are related to destabilization of the substrate-bound HSP90 heteroprotein complex. Even though gamendazole produced a decline in AKT1 and ERBB2, no accompanying

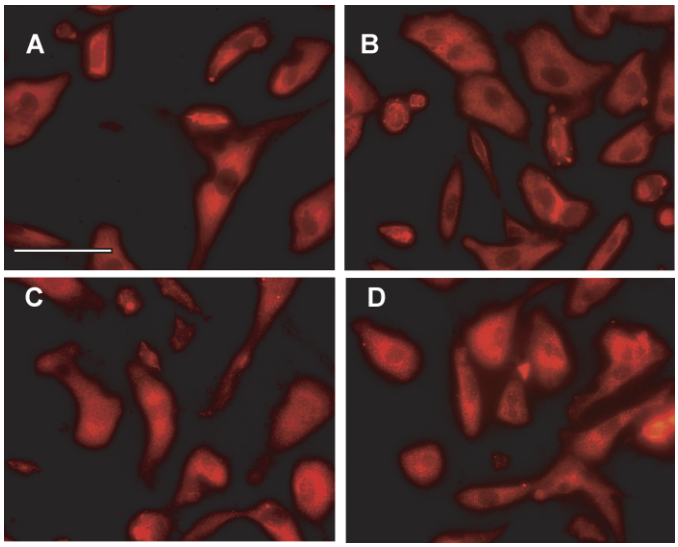

FIG. 9. Immunohistochemistry of HSP90AB1 and EEF1A1 in primary Sertoli cells is not altered by gamendazole. Immunohistochemistry of HSP90AB1 in primary mouse Sertoli cells incubated for 24 h in the absence (**A**) or presence (**B**) of gamendazole is shown. Immunohistochemistry of EEF1A1 in primary mouse Sertoli cells incubated for 24 h in the absence (**C**) or presence (**D**) of gamendazole also is shown. Bar = 50 μm.

increase in HSP90 was observed, suggesting that gamendazole is not dismantling the HSP90-HSF1 heteroprotein complex and, thus, is not inducing the expression of the inducible form of HSP90, HSP90AA1. Because most HSP90 drugs induce HSP90AA1 synthesis, it was important to examine the possibility that localization changes might occur, because Western blots indicated no change in levels of the protein in MCF-7 cells. Immunofluorescence analysis of primary Sertoli cells treated with gamendazole also demonstrated no change in the localization or level of HSP90AB1 or EEF1A1 (Fig. 9). In addition, no change in EEF1A1 levels or localization was observed (Fig. 9). Similar diffuse cytoplasmic patterns of distribution for HSP90 and EEF1A1 have been reported previously [31–33].

Gamendazole Inhibits HSP90-Dependent Luciferase Refolding In Vitro and Proliferation of MCF-7 Cells

The refolding of thermally denatured firefly luciferase in rabbit reticulocyte lysate is an HSP90-dependent process. We recently demonstrated that this is a robust, reproducible assay capable of identifying inhibitors of HSP90 that bind at the N- or C-terminus. Gamendazole inhibited the refolding of denatured luciferase in this assay (IC_{50}, 330 ± 38 μM), demonstrating its ability to functionally inhibit HSP90 activity (Fig. 10A). The IC_{50} for novobiocin (552 ± 12 μM [SD]) was higher than that previously estimated in our high-throughput screen (~400 μM); however, slight differences in lysate batches and experimental conditions could explain this effect [21].

Lonidamine, from which gamendazole was designed, was initially developed as an anticancer therapeutic agent [4]. Because gamendazole displays inhibitory affects on HSP90 client proteins similar to those of other HSP90 anticancer agents, we examined whether gamendazole inhibits proliferation of MCF-7 cells in vitro (Fig. 10B). The IC_{50} for inhibition of MCF-7 cell proliferation by gamendazole was 101 ± 4 μM. For novobiocin, the IC_{50} was more than 2-fold higher (224 ± 5 μM [SD]).

Gamendazole Does Not Bind to the Nucleotide Pocket of TEF1

Two known functions of EEF1A1 and TEF1 are elongation during protein synthesis [34] and actin bundling [35]. The canonical translation function requires exchange of GDP and GTP in a nucleotide-binding pocket of the protein, whereas actin bundling is nucleotide independent. To determine the effect of gamendazole on nucleotide-binding affinities of TEF1, the K_d value of TEF1 for mant-GDP and mant-GMPPNP was measured in the presence of drug at a concentration of 50 μM (Fig. 11). The K_d value of TEF1 for mant-GDP in the absence of drug is 0.18 μM [22]. Stopped-flow kinetics using mant-GDP showed that TEF1 binds to mant-GDP in the presence of the gamendazole with a similar affinity ($K_d = 0.12$). The K_d value of TEF1 for mant-GMPPNP with and without gamendazole was determined as 0.43 and 0.52 μM, respectively. The similar K_d values indicate that

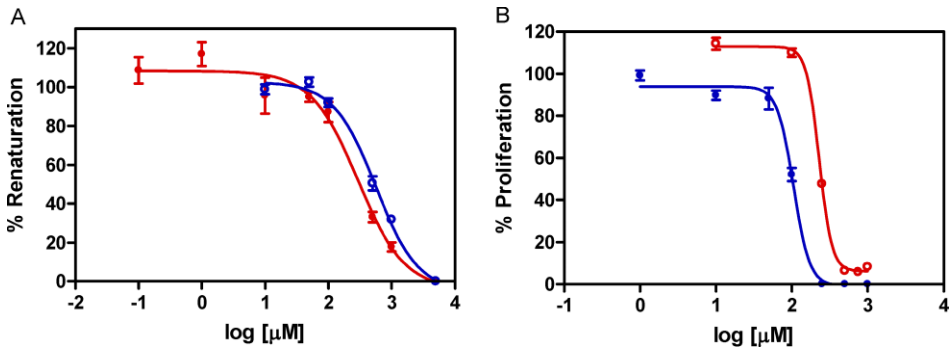

FIG. 10. Effect of HSP90 inhibition on the renaturation of firefly luciferase in rabbit reticulocyte lysate and cell proliferation. **A**) The ability of gamendazole (closed circles) and novobiocin (open circles) to inhibit the HSP90-mediated refolding of thermally denatured firefly luciferase was determined as described previously. Values represent the mean ± SEM for one representative experiment performed in triplicate. Assays were replicated three times, and the IC_{50} of novobiocin correlated well with previously published values. **B**) MCF-7 cells were incubated with gamendazole (closed circles) or novobiocin (open circles) at varying concentrations. Viable cells were quantitated as described in *Materials and Methods*. Values represent the mean ± SEM for one representative experiment performed in triplicate. Assays were replicated three times, and the IC_{50} of novobiocin correlated well with previously published values [75].

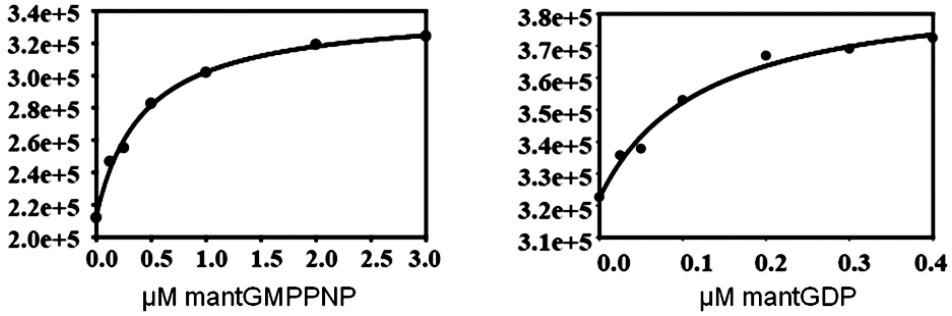

FIG. 11. TEF1 nucleotide-binding assay. Aliquots of mant-GMPPNP (**A**) and mant-GDP (**B**) were added to the binding buffer and TEF1 (1 μM) with 50 μM gamendazole. The fluorescence was measured by fluorescence resonance energy transfer via excitation at 280 nm and emission of 440 nm for the mant moiety. Data was fit to a hyperbolic curve to give a K_d value.

gamendazole does not affect nucleotide-binding properties of EEF1A1.

Gene Transcription Changes Elicited by Gamendazole

The data reported here represent, to our knowledge, the first reported gene microarray studies for LND, gamendazole, or any other ICA of this type. Gene microarray analysis of testis from rats given a single dose of gamendazole or LND revealed important clues regarding the mechanism of action of gamendazole. The purpose of the experiment was to determine differences in the temporal pattern and identity of genes that respond to gamendazole versus LND at the lowest doses that cause complete loss of spermatids and infertility and, thus, to distinguish the earliest responses related to the loss of spermatids.

Table 1 summarizes a subset of data for selected genes related to Sertoli cell-spermatogenic junctions that showed a significant change relative to time-matched controls. (The complete gene microarray data set is available at http://www.ncbi.nlm.nih.gov/geo/ in series record GSE8485.)

It should be noted that the top four upregulated genes in the table also were the most dramatically altered of all the known genes identified in the microarray analysis. Genes known to be involved in the maintenance of Sertoli cell-spermatid junctions were found to change more rapidly with treatment using gamendazole as compared to treatment using LND (Table 1). Notably, gamendazole elicited a significant increase in three testis interleukin 1 genes (between 5- and 14-fold) at the earliest time point (4 h) after treatment of rats with gamendazole. The rapid increase in multiple interleukin 1 gene transcripts is consistent with the dramatic increase in testicular gro1 expression. Gro1 showed the largest increase in transcription of all the upregulated genes. Interleukin 1 increases gro1 through both NFKB-dependent and -independent mechanisms [36]. Mitogen-activated protein (MAP) kinase phosphatase also was increased more rapidly by gamendazole compared to LND. The MAP kinase phosphatase downregulates MAP kinase, causing degradation of the junctions and release of spermatids [37], an effect noted for both antispermatogenic agents. *Nfkbia* also was upregulated more rapidly by gamendazole compared to LND. NFKB has a protective role concerning junction integrity [38]. The rapid upregulation of *Nfkbia*, plus the release of *Nfkbia* via disruption of its complex with HSP90, as indicated by the reduction of AKT1 and ERBB2 protein levels (Fig. 8), may augment the rapid upregulation of interleukin 1 genes. These data also show that testin was upregulated by both agents, but at later time points. Testin was shown to be involved in the antispermatogenic response to LND [39]; however, the temporal data here suggest that changes in testin gene transcription may be a secondary rather than a primary response to these contraceptive agents.

With regard to downregulated genes, a decline in Rho also may contribute to disruption of Sertoli cell-spermatid junctions [40]. The dramatic decline in both HSP70.3 and RT1 class 1b suggests that the major histocompatibility complex (MHC) region may be targeted by these leads. This also is worth noting, because HSP90 inhibitors usually cause an upregulation of HSP70 [41, 42]. In RT1 mutants, gonadal development and spermatogenesis are impaired [43]. The important role that the MHC genes play in both pre- and postmeiotic spermatogenesis suggests that a prolonged effect on genes in this complex may be a marker of an undesired effect of contraceptive agents that have reduced reversibility or that the early response to these leads is significant enough to

TABLE 1. Selected testis genes, related to Sertoli cell-spermatid junction disruption altered in response to gamendazole versus LND.[a]

Genes	Gamendazole 4 h vs control fold change	Gamendazole 12 h vs control fold change	Gamendazole 24 h vs control fold change	LND 4 h vs control fold change	LND 12 h vs control fold change	LND 24 h vs control fold change
Gro1 (*Cxcl1*)	85.43	50.81	11.46	39.36	99.68	24.73
Interleukin 1 alpha, splice variant (*Il1a_v1*)	13.63	4.29	4.53	6.57	6.12	6.35
Interleukin 1 alpha (*Il1a*)	12.48	9.41	4.4	6.76	13.88	6.55
Interleukin 1 beta (*Il1b*)	5.15	2.81	ND	ND	2.26	ND
MAP-kinase phosphatase (*Dusp5*)	5.06	5.06	4.34	2.42	4.04	5.49
IKBA_RAT NF-kappaB inhibitor alpha (*Nfkbia*)	4.4	1.87	1.25	3.2	2.22	1.48
Testin	3.24	17.57	52.44	1.83	3.64	30.58
Hsp70–3 (*Hspa1a*)	−10.03	ND	ND	−5.56	ND	ND
Rattus norvegicus RT1 class Ib gene (*Rt1-n1*)	−6.76	−4.75	−2.24	−6.76	−5.61	−3.06
Moderately similar to T30867 Rho-guanine nucleotide exchange factor - mouse (*M. musculus*) (*RGD1565043_predicted*)	−3.8	−1.1	−1.34	−1.69	−1.01	−1.15

[a] The complete gene array data set are available at http://www.ncbi.nlm.nih.gov/geo/ in series record GSE8485; ND, not determined.

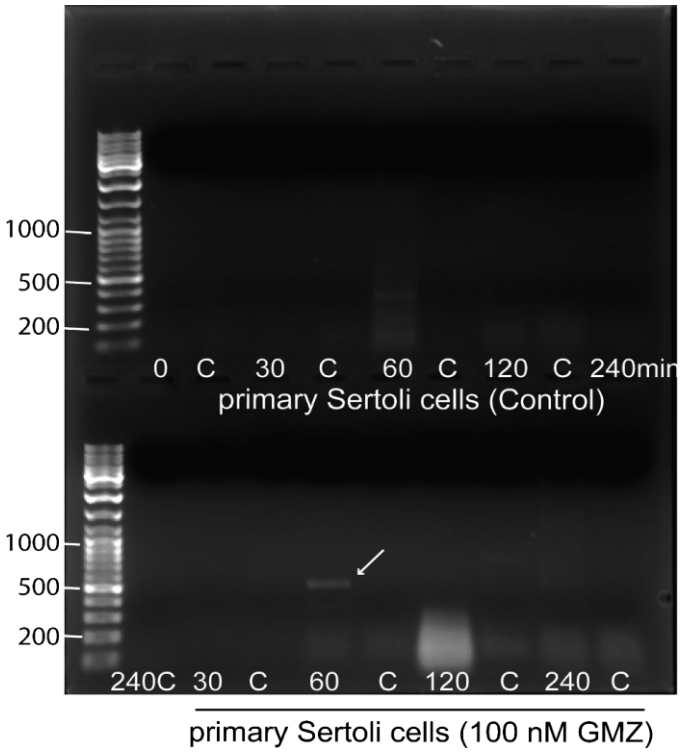

FIG. 12. RT-PCR of *Il1a* in primary Sertoli cells treated with and without gamendazole (GMZ; 10 nM) for 0–240 min.

convert the transcription machinery over to the gamendazole-upregulated genes at the expense of housekeeping genes, such as those associated with the MHC.

*Confirmation of Interleukin 1α (*Il1a*) as an Early Response Gene in Primary Sertoli Cells Treated with Gamendazole*

Il1a is a known disruptor of Sertoli cell-spermatid junction integrity [44], and it has been proposed as an important regulator of Sertoli cell-spermatogenic cell interactions [7]. Three interleukin 1 genes were among the most rapidly and dramatically increased genes in response to gamendazole. The primary hypothesis driving the research is that Sertoli cells are the primary target cell for the antispermatogenic effect of gamendazole. To provide further support for this hypothesis, we confirmed *Il1a* as an early response gene to gamendazole in primary Sertoli cells. We performed RT-PCR using RNA prepared from primary Sertoli cells cultured in the absence and presence of 100 nM gamendazole for 0, 30, 60, 120, and 240 min (Fig. 12). This dose of gamendazole was well within the concentration range used to test LND effects in vitro during previous studies [39]. At 60 min of gamendazole treatment, a spike of amplified product of approximately 500 bp, the size expected for *Il1a*, was observed (Fig. 12). In the absence of gamendazole, no amplified product was detected at any time point. The product also was absent in the reactions performed without added reverse transcriptase (indicated by a C at the lane next to each positive time point in Fig. 12), confirming that the signal was derived from amplified mRNA.

DISCUSSION

We have developed gamendazole [45] and its newer analogue, H2-gamendazole (3-[1-(2,4-dichlorobenzyl)-6-trifluoromethyl-1*H*-indazol-3-yl]-propionic acid), as the most

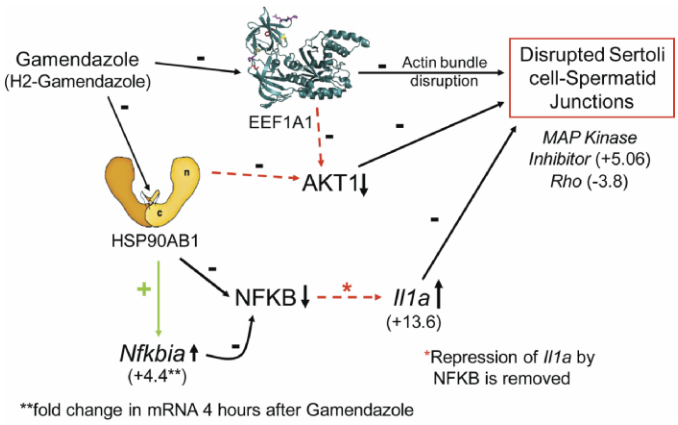

FIG. 13. Proposed mechanism of action of gamendazole relating binding to HSP90AB1 and EEF1A1, gene transcription changes, and disruption of Sertoli cell-spermatid junctions.

potent antispermatogenic analogues of LND synthesized thus far. Because a male contraceptive agent would be used most commonly by otherwise healthy individuals, the successful development of such an agent for human use will require minimal side effects. Therefore, it is wise practice—and our plan—to discover and develop alternative chemical scaffolds that act in a manner similar to that of gamendazole. Thus, an understanding of the mechanism of action of gamendazole is essential to achieve these goals. In the present study, we identified HSP90AB1 and EEF1A1 as novel antispermatogenic male contraceptive targets that bind gamendazole. The identification of HSP90AB1 and EEF1A1 as likely binding targets for gamendazole was demonstrated by multiple functional and binding approaches, including: 1) MALDI-TOF identification and multiple peptide sequence match for these proteins in the gamendazole affinity-purified material from both testis and TM4 cells, 2) gamendazole-dependent elution of protein bands containing EEF1A1 and HSP90AB1 and competition affinity binding from cytosols of testis and Sertoli cells, and 3) identification of bands of similar mass in three separate tissues (testis, TM4 cells, and ovarian cancer cell lines; Western immunoblot analysis confirmed the presence of both of these proteins in the affinity purified bands), 4) the finding that recombinant HSP90 (HSP82) and EEF1A1 as well as TEF1-bound UV-BT-GMZ and could be competed by free gamendazole, 5) the finding that gamendazole inhibited luciferase refolding in a HSP90-dependent process in an in vitro rabbit reticulocyte assay, and 6) the finding that gamendazole treatment downregulates known HSP90 client proteins. Taken together, these results strongly suggest that HSP90AB1 and EEF1A1 may be targets for gamendazole binding that need to be explored in greater detail to the elucidate antispermatogenic mechanism of action of gamendazole. Furthermore, we showed that Sertoli cells respond to gamendazole by rapidly upregulating *Il1a*, a known disruptor of Sertoli cell-spermatid junctional complexes. Finally, based on these observations as well as on supporting observations in the literature, we have developed and proposed a testable model for the antispermatogenic mechanism of action of gamendazole.

Although ICAs like LND had been proposed for exploration as antispermatogenic contraceptives [46, 47], little was known about their binding targets or their precise mechanism of action. Disruption of the Sertoli cell-spermatid junctional complexes is known to occur in response to ICAs [7], including gamendazole, resulting in predominant loss of

spermatids from the seminiferous epithelium [4]. The data presented in this report that HSP90AB1 and EEF1A1 are direct binding targets for gamendazole is a significant new observation. Neither HSP90AB1 nor EEF1A1 were previously proposed as targets for male contraceptive development [2] or identified in mechanistic studies using earlier LND analogues [7].

A concern in the drug development of gamendazole raised by these findings relates to the ubiquitous nature of both HSP90AB1 and EEF1A1. For example, an EST search of the UniGene database for predicted tissue expression for HSP90 homologues suggests that HSP90AB1 has a slightly narrower tissue distribution than HSP90AA1, whereas EEF1A1 expression is broad. Thus, two obvious and related questions are: How can an agent that targets two ubiquitous proteins be used for male contraception or any other purpose, and shouldn't such an agent produce serious side effects? To address these concerns, a number of key points and experimental observations warrant discussion.

The Ubiquitous Nature of HSP90 and EEF1A1

If gamendazole produced broad, prolonged effects on major HSP90 or EEF1A1 functions, we would expect severe toxic side effects during animal studies. With both single-dose oral and i.p. administration, however, and seven consecutive daily dose experiments using doses 4- to 8-fold higher than that required to have a contraceptive effect, no adverse side effects, behavioral changes, or organ histopathology at necropsy were observed [4]. Nonetheless, determinations of toxicity over prolonged periods under conditions for which a male contraceptive likely will be administered are required.

The Problem that HSP90 Knockouts Are Fatal

We propose that gamendazole acts by producing a temporary reduction in function rather than a complete inhibition of its protein targets. In this regard, it is important to note that both HSP90 and EEF1A1 are multifunction proteins and products of multiple genes. Our data demonstrate that gamendazole affects a specific subset of the functions of both of these proteins rather than acting as a broad inhibitor of these proteins.

Regarding HSP90, a temporary reduction in function (as proposed for gamendazole) is very different than a chronic knockout of function. This is supported by the *Drosophila* HSP90 (HSP83) reduction-in-function mutant data that show only a male sterility phenotype whereas HSP90 knockouts are fatal [48]. In this regard, our data demonstrate that gamendazole binds to HSP90AB1 rather than to HSP90AA1. In mammals, at least two isoforms of HSP90, HSP90AA1 and HSP90AB1, are present. Even though the testis contains more HSP90AA1 than HSP90AB1 [49–51], only HSP90AB1 was pulled out of testis and TM4 Sertoli cell cytosols by BT-GMZ. It is worth noting that our in vitro-binding studies used the yeast homologue of HSP90 (HSP82), which actually bears higher homology to HSP90AB1 than to HSP90AA1.

An HSP90 isoform-specific response also is supported by the MCF-7 HSP90 client data (Fig. 8). Even though MCF-7 cells express both isoforms, the downregulation of the HSP90 client proteins ERBB2 and AKT1 was not associated with the upregulation of HSP90. Gamendazole did not elicit the induction of HSP90AA1 and HSP70 normally associated with modulation of the HSP90 heteroprotein complex [41, 42], suggesting the mechanism of action of gamendazole is unique compared to those of other reported HSP90 inhibitors. In this regard, Millson et al. [52] have shown that the ability of HSP90 drugs to affect HSP90 functions is related to the HSP90 isotype specificity.

Regarding EEF1A1, our data demonstrate that gamendazole does have a function-selective interaction, in that no effect of gamendazole on nucleotide binding is observed; thus, gamendazole may not affect the protein synthetic role of this protein. Gamendazole does, however, bind directly to the protein and, thus, probably binds to a domain outside of the nucleotide pocket region of the protein [53]. Therefore, a role that EEF1A1 could play in the antispermatogenic effect of gamendazole may be through mechanisms that disrupt Sertoli cell-germ cell junction integrity by disruption of the EEF1A1 bundling of F-actin, a function separable from the elongation role [53–55]. A disruption of actin bundling by gamendazole makes sense, in that actin bundles are a structural component critical to maintaining the ectoplasmic specializations between Sertoli cells and germ cells as well as Sertoli cell-Sertoli cell junctions [7, 56]. A germ cell-specific isoform of EEF1A1 was identified in spermatogonia and spermatocytes in *Xenopus laevis* [57]. Whether these are expressed and functional in testis and whether gamendazole shows a preference of binding of these isoforms remain to be determined.

The Response to Gamendazole Is Rapid and Transient

In addition to a selective inhibition of a subset of functions of HSP90AB1 and EEF1A1, our data suggest that gamendazole may act on the Sertoli cells in a rapid and transient fashion. Primary Sertoli cells incubated in the presence of 100 nM gamendazole showed a brief upregulation of *Il1a* transcription 1 h after compound addition, even though the compound was present during the entire 2-h incubation period. This is matched by similar in vivo transitory upregulation of gene microarray data for three testis interleukin 1 genes and an *Nfkbia* gene. Similarly, animals that showed reversible infertility in response to gamendazole displayed a rapid and brief reduction in circulating inhibin B levels [4]. It should be noted that the pharmacokinetics of LND, which has the same basic chemical scaffold as gamendazole, shows a peak in circulating levels between 0.5 and 4 h after single administration [58, 59]. In data to be published in detail elsewhere, we have found that H2-gamendazole, an analogue of gamendazole with identical contraceptive efficacy and potency, shows oral absorption half-lives more rapid than those of LND (11 and 130 min at 0.5 and 2 mg/kg, respectively) but with low apparent tissue distribution values. In addition, a recent report by Millson et al. [52] demonstrated that differences between HSP90AA1 and HSP90AB1 client protein changes are related to different sensitivities of the HSP90 isotypes to inhibitors. We conclude from these observations that the reversibility of these compounds and lack of side effects depends not only on the specificity of the targets but also on the pharmacokinetic and tissue uptake profiles. In other words, the results could be explained by low tissue distribution and/or preferential absorption by the testis. In addition, the relative affinity and tissue distribution of HSP90AB1 versus EEF1A1 may be a contributing factor to the lack of side effects observed so far. Higher doses and longer half-life or tissue retention may cause poor reversibility because of disruption of a wider spectrum of Sertoli cell-germ cell junctions more basal than the apical ectoplasmic specializations, including, in the worst-case scenario, the blood-testis barrier [60]. In this regard, extensive tissue uptake, distribution, metabolism, and pharmacokinetic studies will be undertaken to determine the answers to these questions.

A Testable Model for the Antispermatogenic Mechanism of Action of Gamendazole

The HSP90 and EEF1A1 interactions and gene transcription changes in response to gamendazole have provided insights regarding the pathways involved in signal transduction between gamendazole binding to its target proteins and the disruption of spermatogenesis. Based on our observations and on the results of studies in the literature, we offer a testable model for the mechanism of action of gamendazole (Fig. 13). Several HSP90-associated pathways are known to be coupled to the disruption of Sertoli cell-spermatid junctional complexes. A well-known client of HSP90, AKT1, is involved in maintaining the integrity of the Sertoli cell-spermatid junctions [61]. In addition, AKT12 is a binding partner of EEF1A1 [62], and gamendazole could contribute to the decline of AKT1 by a similar mechanism. We showed that gamendazole treatment causes degradation of AKT1. NFKB has a protective role on Sertoli cell junction integrity [38]. Pharmacologic agents that disrupt HSP90 disrupt NFKB, probably via release of the NFKBIA complex [63–65]. In our experiments, gamendazole produced a decline in AKT1 and ERBB2 protein levels, which is consistent with a downregulation of NFKB. *Nfkbia* transcription in the testis, in particular, was significantly higher 4 h after gamendazole administration, which also will synergize the downregulation of NFKB activity. In a second and related pathway, ICAs are known to increase inflammatory cytokines, such as interleukins and tumor necrosis factor, which also disrupt Sertoli cell junctions [7]. We found that several interleukin 1 genes were significantly elevated in testis 4 h after gamendazole administration. This also was confirmed by RT-PCR of *Il1a* in primary Sertoli cells treated with gamendazole. In this regard, inactivation of NFKB by NFKBIA stimulates interleukin 1 expression [66, 67]. An increase in interleukin 1 expression could explain the observed decline in inhibin B production by Sertoli cells in response to extremely low concentrations of gamendazole [4, 68]. In addition to disruption of Sertoli cell-spermatogenic cell junctions, other reported effects of LND analogues could be caused by disruption of testicular HSP90 functions, including apoptosis of late-stage spermatogenic cells [69] and disruption of mitotic spindle components [70]. Our gene transcription data for both gamendazole and LND, however, suggests that the genes involved in these processes occur after the initial changes highlighted in Table 1 and probably are secondary effects or beyond. The complete gene microarray data set is available online at http://www.ncbi.nlm.nih.gov/geo/ in series record GSE8485.

Similarly, the role that EEF1A1 could play in the antispermatogenic effect of gamendazole also may be via disruption of apical ectoplasmic specialization junction integrity (Fig. 13) through cytoskeletal interactions involving inhibition of EEF1A1 bundling of F-actin [53–55]. Another EEF1A1 inhibitor, the anticancer flavonoid quercetin, causes infertility in male rats and mice after oral administration [71]. Quercetin inhibits EEF1A1 by direct binding and inhibition of the protein synthetic function of this protein [72–74]. In studies carried out in our laboratory, however, administration of quercetin under the same conditions that caused infertility in rats and mice [71] produced no effect on spermatogenesis (data not shown). Because gamendazole likely does not bind to the nucleotide-binding region of EEF1A1, the lack of an effect of quercetin on spermatogenesis is consistent with our suggestion that other functions of EEF1A1, such as actin bundling, are more critical to the observed loss of spermatids via disruption of actin-filament bundles related to Sertoli cell-spermatid ectoplasmic specialization junctions.

Even though the primary action of gamendazole appears to involve loss of spermatids, it is possible that the failure of some animals to regain fertility [4] results from interactions of gamendazole with EEF1A1 and/or HSP90 involving Sertoli cell interactions with earlier-stage spermatogenic cells. This is an important driving force for testing the proposed model of gamendazole action. In this regard, future experiments will need to determine whether 1) gamendazole exerts it reversible inhibition of spermatogenesis via HSP90AB1, EEF1A1, or both; 2) what mechanisms distinguish reversible from irreversible effects of this class of orally active antispermatogenic lead agents; and 3) the structure and atomic interaction that define the docking site of gamendazole within HSP90AB1 and EEF1A1. Future experiments then must use this structural information to design and discover new chemical scaffolds as leads for antispermatogenic agents.

ACKNOWLEDGMENTS

The authors wish to acknowledge the excellent technical support of Michael J. Wulser, Sotirios E. Macheras, and summer medical students Kimberly Pickens, Adam Gregg, Melissa K. Emerson, and Brent Burroughs. The authors also wish to thank Drs. Michael Alterman, Todd Williams, and Nadezhda Anatolyevna Galeva of the Biochemical Research Service Laboratory at the University of Kansas for processing and analyzing samples by MALDI-TOF mass spectrometry; Kathy Roby of the University of Kansas Medical Center for the ID8 ovarian cancer cells, and Clark Bloomer and Stan Svojanovsky of the University of Kansas Medical Center Microarray Core for assistance with running and analyzing the gene microarray data. Thanks to Dr. Hyun Kim, Contraception and Reproductive Health Branch, National Institute of Child Health and Human Development, for advice and support.

REFERENCES

1. DePaolo LV, Hinton BT, Braun RE. Male contraception: Views to the 21st Century, Bethesda, MD, USA, 9–10 September 1999. Trends Endocrinol Metab 2000; 11:66–68.
2. Nass SJ, Strauss JF III (eds.). New Frontiers in Contraceptive Research: A Blueprint for Action. Washington, DC: National Academies Press; 2004.
3. Waites GM. Development of methods of male contraception: impact of the World Health Organization Task Force. Fertil Steril 2003; 80:1–15.
4. Tash JS, Attardi B, Hild SA, Chakrasali R, Jakkaraj SR, Georg GI. A novel potent indazole carboxylic acid derivative blocks spermatogenesis and is contraceptive in rats after a single oral dose. Biol Reprod 2008; 78: 1127–1138.
5. Coulston F, Dougherty WJ, LeFevre R, Abraham R, Silvestrini B. Reversible inhibition of spermatogenesis in rats and monkeys with a new class of indazol-carboxylic acids. Exp Mol Pathol 1975; 23:357–366.
6. De Martino C, Malcorni W, Bellocci M, Floridi A, Marcante ML. Effects of AF 1312 TS and lonidamine on mammalian testis. A morphological study. Chemotherapy 1981; 27(suppl 2):27–42.
7. Mruk DD, Cheng CY. Sertoli-Sertoli and Sertoli-germ cell interactions and their significance in germ cell movement in the seminiferous epithelium during spermatogenesis. Endocr Rev 2004; 25:747–806.
8. Heywood R, James RW, Scorza Barcellona P, Campana A, Cioli V. Toxicological studies on 1-substituted-indazole-3-carboxylic acids. Chemotherapy 1981; 27(suppl 2):91–97.
9. Robustelli della Cuna G, Pedrazzoli P. Toxicity and clinical tolerance of lonidamine. Semin Oncol 1991; 18:18–22.
10. Delfino FJ, Walker WH. NF-κB induces cAMP-response element-binding protein gene transcription in Sertoli cells. J Biol Chem 1999; 274:35607–35613.
11. Mather JP. Establishment and characterization of two distinct mouse testicular epithelial cell lines. Biol Reprod 1980; 23:243–252.
12. Shevchenko A, Wilm M, Vorm O, Mann M. Mass spectrometric sequencing of proteins silver-stained polyacrylamide gels. Anal Chem 1996; 68:850–858.
13. Roby KF, Taylor CC, Sweetwood JP, Cheng Y, Pace JL, Tawfik O, Persons DL, Smith PG, Terranova PF. Development of a syngeneic mouse model for events related to ovarian cancer. Carcinogenesis 2000; 21: 585–591.

14. Son DS, Roby KF, Rozman KK, Terranova PF. Estradiol enhances and estriol inhibits the expression of CYP1A1 induced by 2,3,7,8-tetrachlorodibenzo-*p*-dioxin in a mouse ovarian cancer cell line. Toxicology 2002; 176:229–243.
15. Candiano G, Bruschi M, Musante L, Santucci L, Ghiggeri GM, Carnemolla B, Orecchia P, Zardi L, Righetti PG. Blue silver: a very sensitive colloidal Coomassie G-250 staining for proteome analysis. Electrophoresis 2004; 25:1327–1333.
16. Richter K, Muschler P, Hainzl O, Buchner J. Coordinated ATP hydrolysis by the Hsp90 dimer. J Biol Chem 2001; 276:33689–33696.
17. Anand M, Balar B, Ulloque R, Gross SR, Kinzy TG. Domain and nucleotide dependence of the interaction between *Saccharomyces cerevisiae* translation elongation factors 3 and 1A. J Biol Chem 2006; 281:32318–32326.
18. Carr-Schmid A, Pfund C, Craig EA, Kinzy TG. Novel G-protein complex whose requirement is linked to the translational status of the cell. Mol Cell Biol 2002; 22:2564–2574.
19. Yu XM, Shen G, Neckers L, Blake H, Holzbeierlein J, Cronk B, Blagg BSJ. Hsp90 inhibitors identified from a library of novobiocin analogues. J Am Chem Soc 2005; 127:12778–12779.
20. Shen G, Blagg BS. Radester, a novel inhibitor of the Hsp90 protein folding machinery. Org Lett 2005; 7:2157–2160.
21. Galam L, Hadden MK, Ma Z, Ye QZ, Yun BG, Blagg BS, Matts RL. High-throughput assay for the identification of Hsp90 inhibitors based on Hsp90-dependent refolding of firefly luciferase. Bioorg Med Chem 2007; 15:1939–1946.
22. Pittman YR, Valente L, Jeppesen MG, Andersen GR, Patel S, Kinzy TG. Mg^{2+} and a key lysine modulate exchange activity of eukaryotic translation elongation factor 1Bα. J Biol Chem 2006; 281:19457–19468.
23. Rosenfeld J, Capdevielle J, Guillemot JC, Ferrara P. In-gel digestion of proteins for internal sequence analysis after one- or two-dimensional gel electrophoresis. Anal Biochem 1992; 203:173–179.
24. Nishida T, Nishino N, Takano M, Sekiguchi Y, Kawai K, Mizuno K, Nakai S, Masui Y, Hirai Y. Molecular cloning and expression of rat interleukin-1α cDNA. J Biochem (Tokyo) 1989; 105:351–357.
25. Jonsson CK, Zetterstrom RH, Holst M, Parvinen M, Soder O. Constitutive expression of interleukin-1α messenger ribonucleic acid in rat Sertoli cells is dependent upon interaction with germ cells. Endocrinology 1999; 140: 3755–3761.
26. Neckers L, Neckers K. Heat-shock protein 90 inhibitors as novel cancer chemotherapeutics—an update. Expert Opin Emerg Drugs 2005; 10:137–149.
27. Lamberti A, Caraglia M, Longo O, Marra M, Abbruzzese A, Arcari P. The translation elongation factor 1A in tumorigenesis, signal transduction, and apoptosis: review article. Amino Acids 2004; 26:443–448.
28. Sausville EA, Elsayed Y, Monga M, Kim G. Signal transduction—directed cancer treatments. Annu Rev Pharmacol Toxicol 2003; 43: 199–231.
29. Marcu MG, Chadli A, Bouhouche I, Catelli M, Neckers LM. The heat shock protein 90 antagonist novobiocin interacts with a previously unrecognized ATP-binding domain in the carboxyl terminus of the chaperone. J Biol Chem 2000; 275:37181–37186.
30. Zhang H, Burrows F. Targeting multiple signal transduction pathways through inhibition of Hsp90. J Mol Med 2004; 82:488–499.
31. Tuohimaa P, Pekki A, Blauer M, Joensuu T, Vilja P, Ylikomi T. Nuclear progesterone receptor is mainly heat shock protein 90-free in vivo. Proc Natl Acad Sci U S A 1993; 90:5848–5852.
32. Pekki AK. Different immunoelectron microscopic locations of progesterone receptor and HSP90 in chick oviduct epithelial cells. J Histochem Cytochem 1991; 39:1095–1101.
33. Kjaer S, Wind T, Ravn P, Ostergaard M, Clark BF, Nissim A. Generation and epitope mapping of high-affinity scFv to eukaryotic elongation factor 1A by dual application of phage display. Eur J Biochem 2001; 268: 3407–3415.
34. Merrick WC, Nyborg J. The protein biosynthesis elongation cycle. In: Hershey JWB, Mathews MB (eds.), Translational Control of Gene Expression: Cold Spring Harbor, NY: Cold Spring Harbor Laboratory; 2000:89–126.
35. Demma M, Warren V, Hock R, Dharmawardhane S, Condeelis J. Isolation of an abundant 50 000-dalton actin filament bundling protein from *Dictyostelium amoebae*. J Biol Chem 1990; 265:2286–2291.
36. Loukinova E, Chen Z, Van Waes C, Dong G. Expression of proangiogenic chemokine Gro 1 in low and high metastatic variants of Pam murine squamous cell carcinoma is differentially regulated by IL-1aα, EGF, and TGF-β1 through NF-κB dependent and independent mechanisms. Int J Cancer 2001; 94:637–644.
37. Zhang J, Wong CH, Xia W, Mruk DD, Lee NP, Lee WM, Cheng CY. Regulation of Sertoli-germ cell adherens junction dynamics via changes in protein-protein interactions of the N-cadherin-β-catenin protein complex, which are possibly mediated by c-Src and myotubularin-related protein 2: an in vivo study using an androgen suppression model. Endocrinology 2005; 146:1268–1284.
38. Brown RC, Mark KS, Egleton RD, Huber JD, Burroughs AR, Davis TP. Protection against hypoxia-induced increase in blood-brain barrier permeability: role of tight junction proteins and NFKB. J Cell Sci 2003; 116:693–700.
39. Grima J, Zhu L, Cheng CY. Testin is tightly associated with testicular cell membrane upon its secretion by Sertoli cells whose steady-state mRNA level in the testis correlates with the turnover and integrity of intertesticular cell junctions. J Biol Chem 1997; 272:6499–6509.
40. Lui WY, Mruk DD, Cheng CY. Interactions among IQGAP1, Cdc42, and the cadherin/catenin protein complex regulate Sertoli-germ cell adherens junction dynamics in the testis. J Cell Physiol 2005; 202:49–66.
41. Ansar S, Burlison JA, Hadden MK, Yu XM, Desino KE, Bean J, Neckers L, Audus KL, Michaelis ML, Blagg BS. A nontoxic Hsp90 inhibitor protects neurons from Aβ-induced toxicity. Bioorg Med Chem Lett 2007; 17:1984–1990.
42. Csermely P, Schnaider T, Soti C, Prohaszka Z, Nardai G. The 90-kDa molecular chaperone family: structure, function, and clinical applications. A comprehensive review. Pharmacol Ther 1998; 79:129–168.
43. Kunz HW, Gill TJ III, Dixon BD, Taylor FH, Greiner DL. Growth and reproduction complex in the rat. Genes linked to the major histocompatibility complex that affect development. J Exp Med 1980; 152:1506–1518.
44. Nilsson M, Husmark J, Bjorkman U, Ericson LE. Cytokines and thyroid epithelial integrity: interleukin-1α induces dissociation of the junctional complex and paracellular leakage in filter-cultured human thyrocytes. J Clin Endocrinol Metab 1998; 83:945–952.
45. Georg GI, Tash JS, Chakrasali R, Jakkaraj SR (inventors). Lonidamine analogues and their use in male contraception and cancer treatment. US Patent application document no. 20060047126; 2006.
46. Cheng CY, Mo M, Grima J, Saso L, Tita B, Mruk D, Silvestrini B. Indazole carboxylic acids in male contraception. Contraception 2002; 65: 265–268.
47. Gatto MT, Tita B, Artico M, Saso L. Recent studies on lonidamine, the lead compound of the antispermatogenic indazol-carboxylic acids. Contraception 2002; 65:277–278.
48. Yue L, Karr TL, Nathan DF, Swift H, Srinivasan S, Lindquist S. Genetic analysis of viable Hsp90 alleles reveals a critical role in *Drosophila* spermatogenesis. Genetics 1999; 151:1065–1079.
49. Vamvakopoulos NO. Tissue-specific expression of heat shock proteins 70 and 90: potential implication for differential sensitivity of tissues to glucocorticoids. Mol Cell Endocrinol 1993; 98:49–54.
50. Gruppi CM, Zakeri ZF, Wolgemuth DJ. Stage and lineage-regulated expression of two hsp90 transcripts during mouse germ cell differentiation and embryogenesis. Mol Reprod Dev 1991; 28:209–217.
51. Huang SY, Tam MF, Hsu YT, Lin JH, Chen HH, Chuang CK, Chen MY, King YT, Lee WC. Developmental changes of heat-shock proteins in porcine testis by a proteomic analysis. Theriogenology 2005; 64:1940–1955.
52. Millson SH, Truman AW, Racz A, Hu B, Panaretou B, Nuttall J, Mollapour M, Soti C, Piper PW. Expressed as the sole Hsp90 of yeast, the α and β isoforms of human Hsp90 differ with regard to their capacities for activation of certain client proteins, whereas only Hsp90β generates sensitivity to the Hsp90 inhibitor radicicol. FEBS J 2007; 274:4453–4463.
53. Gross SR, Kinzy TG. Translation elongation factor 1A is essential for regulation of the actin cytoskeleton and cell morphology. Nat Struct Mol Biol 2005; 12:772–778.
54. Izawa T, Fukata Y, Kimura T, Iwamatsu A, Dohi K, Kaibuchi K. Elongation factor-1α is a novel substrate of rho-associated kinase. Biochem Biophys Res Commun 2000; 278:72–78.
55. Munshi R, Kandl KA, Carr-Schmid A, Whitacre JL, Adams AE, Kinzy TG. Overexpression of translation elongation factor 1A affects the organization and function of the actin cytoskeleton in yeast. Genetics 2001; 157:1425–1436.
56. Mruk DD, Cheng CY. Cell-cell interactions at the ectoplasmic specialization in the testis. Trends Endocrinol Metab 2004; 15:439–447.
57. Abdallah B, Hourdry J, Krieg PA, Denis H, Mazabraud A. Germ cell-specific expression of a gene encoding eukaryotic translation elongation factor 1α (eEF-1α) and generation of eEF-1α retropseudogenes in *Xenopus laevis*. Proc Natl Acad Sci U S A 1991; 88:9277–9281.
58. Newell DR, Mansi J, Hardy J, Button D, Jenns K, Smith IE, Picollo R, Catanese B. The pharmacokinetics of oral lonidamine in breast and lung cancer patients. Semin Oncol 1991; 18:11–17.

59. Grippa E, Gatto MT, Leone MG, Tita B, Adbel-Haq H, Vitalone A, Silvestrini B, Saso L. Analysis of lonidamine in rat serum and testis by high-performance liquid chromatography. Biomed Chromatogr 2001; 15: 1–8.
60. Lee NP, Cheng CY. Ectoplasmic specialization, a testis-specific cell-cell actin-based adherens junction type: is this a potential target for male contraceptive development? Hum Reprod Update 2004; 10:349–369.
61. Siu MK, Wong CH, Lee WM, Cheng CY. Sertoli-germ cell anchoring junction dynamics in the testis are regulated by an interplay of lipid and protein kinases. J Biol Chem 2005; 280:25029–25047.
62. Lau J, Castelli LA, Lin EC, Macaulay SL. Identification of elongation factor 1α as a potential associated binding partner for Akt2. Mol Cell Biochem 2006; 286:17–22.
63. Pittet JF, Lee H, Pespeni M, O'Mahony A, Roux J, Welch WJ. Stress-induced inhibition of the NF-κB signaling pathway results from the insolubilization of the IκB kinase complex following its dissociation from heat shock protein 90. J Immunol 2005; 174:384–394.
64. Lewis J, Devin A, Miller A, Lin Y, Rodriguez Y, Neckers L, Liu ZG. Disruption of hsp90 function results in degradation of the death domain kinase, receptor-interacting protein (RIP), and blockage of tumor necrosis factor-induced nuclear factor-κB activation. J Biol Chem 2000; 275: 10519–10526.
65. Broemer M, Krappmann D, Scheidereit C. Requirement of Hsp90 activity for IκB kinase (IKK) biosynthesis and for constitutive and inducible IKK and NF-κB activation. Oncogene 2004; 23:5378–5386.
66. Nakajima K, Matsushita Y, Tohyama Y, Kohsaka S, Kurihara T. Differential suppression of endotoxin-inducible inflammatory cytokines by nuclear factor κB (NFκB) inhibitor in rat microglia. Neurosci Lett 2006; 401:199–202.
67. O'Gorman MT, Jatoi NA, Lane SJ, Mahon BP. IL-1β and TNF-α induce increased expression of CCL28 by airway epithelial cells via an NFκB-dependent pathway. Cell Immunol 2005; 238:87–96.
68. Okuma Y, Saito K, O'Connor AE, Phillips DJ, de Kretser DM, Hedger MP. Reciprocal regulation of activin A and inhibin B by interleukin-1 (IL-1) and follicle-stimulating hormone (FSH) in rat Sertoli cells in vitro. J Endocrinol 2005; 185:99–110.
69. Maloney A, Workman P. HSP90 as a new therapeutic target for cancer therapy: the story unfolds. Expert Opin Biol Ther 2002; 2:3–24.
70. Glover DM. Polo kinase and progression through M phase in *Drosophila*: a perspective from the spindle poles. Oncogene 2005; 24:230–237.
71. Aravindakshan M, Chauhan PS, Sundaram K. Studies on germinal effects of quercetin, a naturally occurring flavonoid. Mutat Res 1985; 144:99–106.
72. Galasinski W, Chlabicz J, Paszkiewicz-Gadek A, Marcinkiewicz C, Gindzienski A. The substances of plant origin that inhibit protein biosynthesis. Acta Pol Pharm 1996; 53:311–318.
73. Galasinski W. Eukaryotic polypeptide elongation system and its sensitivity to the inhibitory substances of plant origin. Proc Soc Exp Biol Med 1996; 212:24–37.
74. Marcinkiewicz C, Galasinski W, Gindzienski A. EF-1α is a target site for an inhibitory effect of quercetin in the peptide elongation process. Acta Biochim Pol 1995; 42:347–350.
75. Burlison JA, Blagg BS. Synthesis and evaluation of coumermycin A1 analogues that inhibit the Hsp90 protein folding machinery. Org Lett 2006; 8:4855–4858.